Quaternary Science Reviews 238 (2020) 106328

Contents lists available at ScienceDirect

Quaternary Science Reviews

journal homepage: www.elsevier.com/locate/quascirev

Timing and structure of vegetation, fire, and climate changes on the Pacific slope of northwestern Patagonia since the last glacial termination

Patricio I. Moreno

Millennium Nucleus Paleoclimate, Center for Climate Research and Resilience, Institute of Ecology and Biodiversity, Department of Ecological Sciences, Universidad de Chile, Santiago, Chile

ARTICLE INFO

Article history:
Received 19 March 2020
Received in revised form
21 April 2020
Accepted 24 April 2020
Available online 18 May 2020

ABSTRACT

By virtue of its location in the southern mid-latitudes, northwestern Patagonia (40°-44°S) offers the opportunity to unravel the mechanisms involved in the initiation and propagation of paleoclimate signals of hemispheric and global significance. Of particular importance is deciphering the evolution of the Southern Westerly Winds (SWW) considering their influence at continental, zonal, hemispheric, and global scale. Here I present a multi-decadal record from Lago Proschle, a small closed-basin lake located on the Pacific slope of northwestern Patagonia, to examine the timing and structure of vegetation, fire, and climate change along a continuum since the onset of the Last Glacial Termination (T1). The record shows rapid glacier recession during T1, reaching the western Andean foothills in ~400 years or less. *Nothofagus*-dominated forests established between ~17.4–17 ka, followed by closed-canopy North Patagonian Rain Forests (NPRF) with shade-tolerant thermophilous trees between ~16.3–15.4 ka. These changes suggest an abrupt warming trend and an increase in precipitation at ~16.3 ka, associated with a northward shift of the SWW. Subsequent increases in cold-tolerant hygrophilous trees between ~15.4–12.8 ka imply a shift to cold, more humid conditions during the Antarctic Cold Reversal, suggesting stronger SWW influence. This was followed by stand-replacing fires brought by a sudden decline in summer precipitation at ~12.8 ka, associated with a millennial-scale southward shift of the SWW which was contemporaneous with the onset of the Younger Dryas. Dominance of thermophilous, summer-drought tolerant Valdivian rainforest trees and high fire activity ensued between ~10.3–7.8 ka, suggesting peak warmth and overall decline in annual precipitation associated with weakening of the SWW during the early Holocene. A multi-millennial cooling and wetting trend started at ~7.8 ka, brought by stronger SWW influence, followed by recurrent, centennial-scale variations in temperature and precipitation starting at ~6.4 ka. Deforestation, fire, and spread of non-native herbs by Chilean/European settlers began during the late 18th century. Abrupt vegetation changes in the Lago Proschle record were driven by rapid climate changes over the last 17,400 years amplified, in some instances, by fire disturbance.

1. Introduction

Resolving the paleoclimate history of the middle latitudes of the Southern Hemisphere is important for deciphering the mechanisms underlying climate change during the last ice age, its termination, and the current interglacial. This vast region constitutes the interface between polar and tropical climate systems and, thus, is key for examining the initiation and propagation of climate signals of hemispheric and global significance. The Southern Westerly Winds (SWW) exert a permanent influence in the southern mid-latitudes and, in conjunction with the Southern Ocean (SO), establish a coupled system that influences oceanic and atmospheric circulation at regional and global scale, the amount of heat and precipitation that reaches the Antarctic continent, the availability of nutrients in the SO, and the ventilation of CO_2 dissolved in deep waters to the atmosphere via high-latitude upwelling. The timing, structure, and magnitude of paleoclimate events in northwestern Patagonia (40°-44°S) (Fig. 1) offer empirical constraints for unraveling past changes in the SWW, and their

E-mail address: pimoreno@uchile.cl.

https://doi.org/10.1016/j.quascirev.2020.106328
0277-3791/

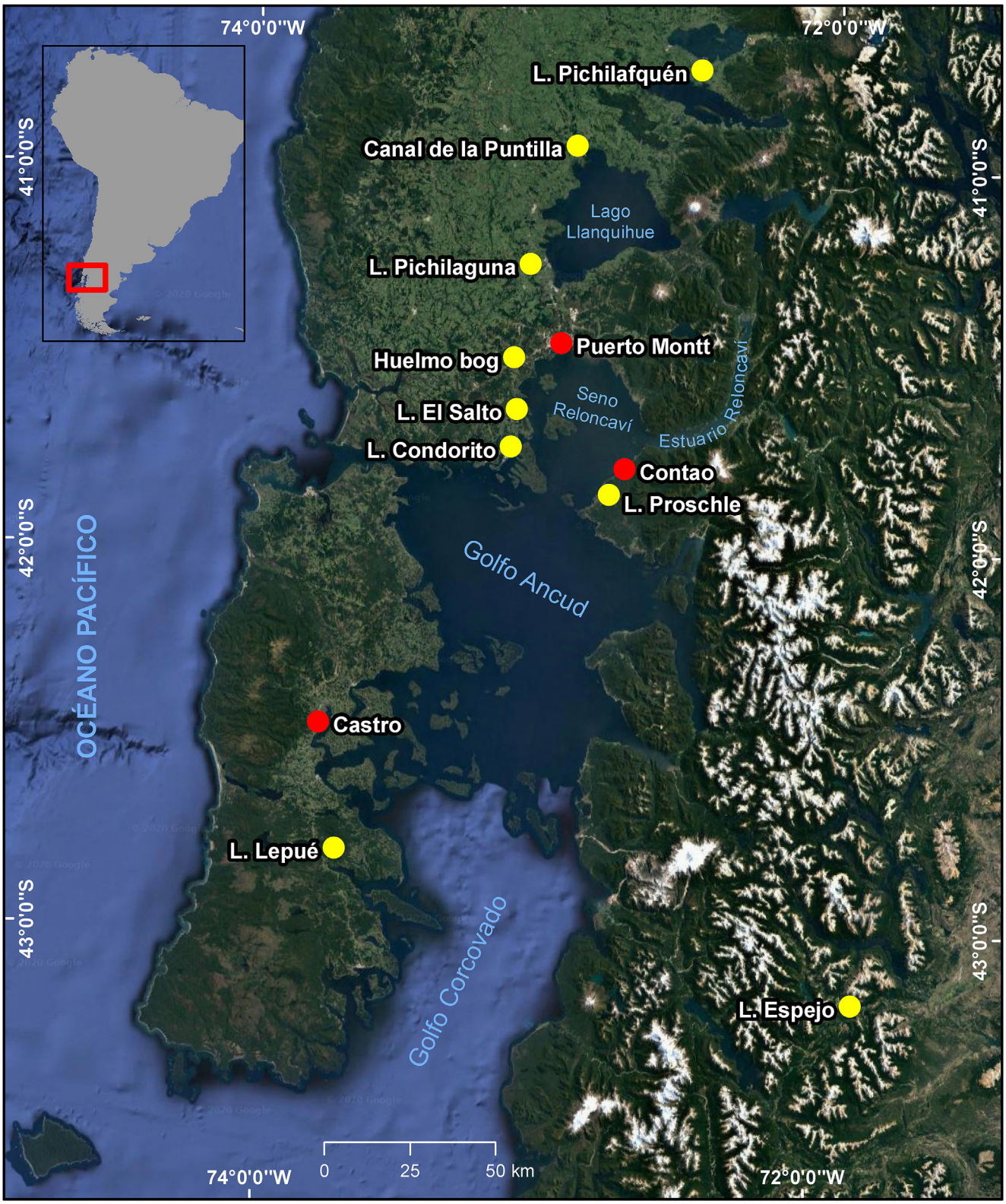

Fig. 1. Satellite image of the Pacific sector of northwestern Patagonian (40°S-44°S) showing the location of Lago Proschle and other sites mentioned in the main text. The Chiloé continental sector corresponds to the western slopes of the Andes that face the Golfo Ancud, Golfo Corcovado, and intervening channels.

relationship with polar and tropical processes since the Last Glacial Maximum (LGM, between ~34 and ~17.8 ka, ka = 1000 calendar years before present).

Geomorphic and stratigraphic studies in northwestern Patagonia indicate that the western LGM margins of piedmont glacier lobes, sourced from the former Patagonian Ice Sheet (PIS), reached modern sea level from ~41°30′S southward (Palacios et al., 2020). Rapid and extensive recession ensued during the Last Glacial

Termination (Termination 1 = T1, between ~17.8 and ~11.7 ka) in response to sustained atmospheric warming, vacating cirques at ~800 m elevation in the Andes in less than 1000 years (Moreno et al., 2015). The exact sequence of environmental changes thereafter has been the subject of discussion in the literature for decades, including the timing and magnitude of climate reversals and glacier readvances during T1, the evolution of SWW influence in the region, and the putative role of humans and fire-regime shifts as drivers of vegetation change. Detailed records on past vegetation and fire activity offer unique insights into the environmental evolution of the Pacific sector of northwestern Patagonia. Considerable achievements over the last ~60 years (Heusser, 1966, 1974; Heusser, 1984; Heusser et al., 1999; Markgraf, 1991; Villagrán, 1985, 1988a, b, 2001) have produced a wealth of information on the vegetation and climate history in the region, documenting -with varying degrees of detail and continuity-the response of plant communities to the major climate transitions through the last glacial-interglacial cycle, the former distribution and composition of plant communities during the LGM, postglacial shifts in plant species distributions, and the potential role of disturbance regimes as drivers of vegetation change. Few records, however, have the chronologic precision, time resolution, and continuity to examine changes in the structure and composition of the vegetation in response to shifts in climate change and disturbance regimes at ecological timescales (<100 years), along a time continuum from T1 to the present.

Here I present a high-resolution, precisely dated and continuous record from Lago Proschle, a small closed-basin lake located on the western Andean foothills of northwestern Patagonia (Fig. 1), to examine the timing and structure of vegetation, fire, and climate change since the onset of T1. I compare these results with similar records from the study area to assess their regional significance and geographic trends, and with paleoclimate records from the southern mid-latitudes and Antarctic ice cores to examine their zonal and hemispheric implications.

1.1. Study area

The Pacific sector of northwestern Patagonia (40°-44°S) features the Chilean Lake District and the Chilotan archipelago, which includes about 40 islands scattered south of Seno Reloncaví to Golfo Corcovado (Fig. 1). The Andes Cordillera establishes the eastern limit of the region, reaches average elevations of ~1800 m.a.s.l. at 40°S, and contains more than 35 isolated glaciers on the highest peaks between 35°S and 45°30′S (Lliboutry, 1998). Volcanism in this region results from the subduction of the Nazca Plate underneath the westward moving South American Plate (Stern, 2004), along a narrow volcanic arc that follows the Liquiñe-Ofqui fault system in Chile between 33° and 46°S. The Southern Andean Volcanic Zone features at least 60 active or potentially active volcanoes in Chile and Argentina, as well as three caldera systems and numerous minor eruptive centers (Stern, 2004). A broad north-south oriented tectonic depression named the Longitudinal Valley occurs between the Coastal Range and the Andes Cordillera in south-central Chile (30°–41°30′S) (Fig. 1). This valley is truncated by the Seno Reloncaví seaway at the latitude of Puerto Montt, transitions south into the interior Chilotan Sea, Golfo de Corcovado, and gives way to the Chonos archipelago further to the south. The Andean sector directly east of the Chilotan archipelago between 41°40′S and 44°S is known as Chiloé Continental, and features a rugged relief with steep-sided glacier valleys blanketed by glacier and volcanic deposits.

Precipitation in northwestern Patagonia is delivered by storms embedded in the SWW and occurs throughout the year, with variations in frontal activity resulting from the seasonal migration of storm tracks (Garreaud et al., 2013). The seasonality of precipitation increases north of 41°S, along with a rise in continentality caused by the rain-shadow effect of the Coastal Range on the Longitudinal Valley (Moreno et al., 2018a). The zone of maximum precipitation (48°- 50°S in central Patagonia) shifts north/south during the winter/summer months, respectively, in concert with latitudinal sea-surface temperature gradients and the interaction between the subtropical Pacific high-pressure cell and the polar low-pressure belt (Aceituno et al., 1993; Garreaud et al., 2013; Quintana and Aceituno, 2012). The Andes Cordillera strongly perturbs the SWW storms: forced ascent of air masses along the windward side of the mountains greatly enhances precipitation in western Patagonia, accompanied by spillover across the Andes and downstream subsidence, generating a marked rain shadow that extends across much of extra-Andean Patagonia (Garreaud et al., 2013). Precipitation over the mid-latitude Pacific Ocean is positively correlated with the intensity of the westerly flow, this correlation increases toward the western coast of South America because of the aforementioned orographic effect, even locations 50–70 km to the east of the Andean divide show a positive correlation between precipitation and zonal wind. The correlation diminishes and turns negative eastward in the extra Andean realm. In addition, the absence of significant orographic barriers in this sector allows the westward penetration of moist easterlies originating from the Atlantic seaboard at times of reduced SWW influence (Agosta et al., 2015).

Interannual precipitation variability in northwestern Patagonia is related to El Niño Southern Oscillation (ENSO) and the Southern Annular Mode (SAM), with negative anomalies in summer precipitation correlated with positive anomalies in these indices. Summer temperature anomalies, on the other hand, are positively correlated with SAM at regional scale (Villalba et al., 2012). Positive departures of the SAM, i.e. anomalously warm and dry summers, generate conditions conducive for wildfire occurrence along western Patagonia as revealed by climate analyses and tree ring-data spanning several centuries (Holz and Veblen, 2012).

The temperate high-rainfall regime of northwestern Patagonia sustains broadleaved temperate rainforests, which closely follow altitudinal, longitudinal, and latitudinal climate gradients in temperature and precipitation from sea level up to the upper treeline (1000–1200 m.a.s.l.). The structure and floristic composition of the modern vegetation afford modern analogues for interpreting paleovegetation, paleoclimate, and vegetation dynamics based on fossil pollen records. Three modern forest communities have been distinguished on the basis of their floristic composition in northwestern Patagonia: the evergreen Valdivian and North Patagonian rainforests, and Deciduous Subantarctic forests. Although these rainforest communities share many trees, shrubs, epiphytes, woody climbers, lianas, ferns, and bryophytes, the presence of key diagnostic taxa enables their distinction in palynological records (Heusser, 1966; Heusser et al., 1999; Villagrán, 1985, 1988b). The palynomorph *Eucryphia cordifolia/Caldcluvia paniculata* is a characteristic component of Valdivian rainforest (VRF) communities which dominated the lowland sectors and adjacent foothills in northwestern Patagonia prior to historic settlement, where relatively high temperatures and summer precipitation declines are most pronounced. North Patagonian rainforests (NPRF), located in cooler and wetter environments at higher elevations, are distinguishable from the VRF in pollen records by the absence of *Eucryphia cordifolia* and by the presence of cold-resistant hygrophilous conifers of the family Podocarpaceae (*Podocarpus nubigena, Saxegothaea conspicua*) and Cupressaceae (*Fitzroya cupressoides* and *Pilgerodendron uviferum*). Deciduous Subantarctic forests, typically dominated by *Nothofagus pumilio*, occur in sub-alpine environments subject to seasonal snow cover under cold, wet, and windy conditions and thus establish the treeline along western Patagonia.

The broad latitudinal distribution of the Subantarctic forest community throughout western Patagonia reflects its ability to withstand low temperatures (Lara et al., 2005). High Andean vegetation dominates the landscapes above the treeline, located between 1000 and 1200 m.a.s.l. in northwestern Patagonia, and constitutes a sparsely vegetated unit dominated by herbs (Poaceae, Asteraceae, Apiaceae, *Gunnera*), and heath (*Pernettya, Empetrum*), along with isolated trees of the species *Nothofagus antarctica*. Low temperatures, strong winds, and prolonged and abundant snow cover constitute limiting factors for the occurrence of woodlands and forests in this harsh environment.

Lago Proschle is located east of Seno Reloncaví, on the windward foothills of the northwestern Patagonian Andes (Fig. 1), where the VRF and NPRF communities intermingle in a transitional zone along a latitudinal and bioclimatic gradient.

1.2. Regional paleoclimate background

Glacial geologic studies from the Chilean Lake District and Isla Grande de Chiloé show recurring glacial advances during Marine Isotope Stage 2, from at least ~33.6 until ~17.8 ka, followed by widespread retreat deep into the Andes within the next millennium (Denton et al., 1999a, 1999b; Moreno et al., 2015). Independently dated palynological records indicate cold and wet glacial conditions between ~24 and ~17.8 ka, followed by an abrupt increase in *Nothofagus* trees at ~17.8 ka that marked the onset of rapid warming at the end of the LGM (Moreno et al., 1999, 2015; Moreno and Leon, 2003). The statistically indistinguishable chronologies for these events demonstrate a coherent, virtually instantaneous response of northwestern Patagonian glaciers and terrestrial ecosystems to a decisive warm pulse that triggered T1 in the mid- and high southern latitudes (Denton et al., 1999a). The beginning of T1 also involved a change from hyperhumid to humid conditions (Moreno et al., 2018a; Pesce and Moreno, 2014), signaling a poleward shift of the SWW during the initial ~1400 years of T1.

A northward shift of the SWW ensued at ~16.4 ka, judging from a precipitation rise recorded in sites from northwestern and central-east Andean Patagonia (45°S) (Henríquez et al., 2017; Moreno et al., 2015, 2018a; Pesce and Moreno, 2014; Vilanova et al., 2019), followed by an intensification between ~14.5 and ~13 ka, a southward shift between ~13 and ~11.5 ka, and weakening between ~11.5 and ~7.5 ka (Moreno, 2004; Moreno et al., 2010, 2015; Moreno and Videla, 2016). A multi-millennial trend toward cooler/wetter climate started at ~7.5 ka and has persisted until the present (Moreno, 2004; Moreno and Videla, 2016). The most recent ~5300 years feature the onset of sub-millennial-scale variability, with centennial-scale warm/dry phases centered at ~5.3, ~4.3, ~3.5, ~2.1, ~1.2 ka, and over the last 150 years, that alternate with cool/wet phases (Moreno and Videla, 2016). Marine-based chronologies from the southeast Pacific sector show a sequence of changes that is broadly consistent with the aforementioned terrestrial records. More specifically, marine reconstructions feature the following multi-millennial phases: an northward migration of the SWW during the LGM (between ~22 and ~18 ka), a southward shift during the early Holocene (between ~12 and ~8 ka), and centennial-scale changes over the most recent ~3000 years (Lamy et al., 1999).

Nearly all glacial geologic and palynologic investigations along the Pacific slope of northwestern Patagonia have been carried out in the lowlands, west or near the LGM margins. Hence, little is known about the vegetation, glacial, and environmental evolution on the western Andean foothills upstream from Seno Reloncaví and the Chilotan Sea (Henríquez et al., 2015; Heusser et al., 1992) (Fig. 1). These are interesting sectors for examining the interplay between climatic and non-climatic drivers of vegetation change, considering the proximity of volcanic centers that have been particularly active since T1 (Alloway et al., 2017; Fontijn et al., 2014). Furthermore, because glaciers covered the western slopes of the northwestern Patagonian Andes during the last glaciation, I expect that plant expansion and colonization into the Chiloé Continental region must have taken place, primarily, through a low-elevation north-to south corridor located along the Andean foothills east of Puerto Montt following T1 (Fig. 1). This area, however, contains large lakes (Lago Llanquihue and L. Todos los Santos), seaways (Seno and Estuario Reloncaví, and the interior Chilotan sea) and climatic barriers to dispersal (low temperatures and high precipitation regimes at higher elevations) which may have imposed restrictions to the eastward and subsequent southward migration of land biota, formerly distributed west of the northwestern Patagonian ice margins. The efficacy of this narrow corridor for the terrestrial biota was dependent upon glacier extent and volcanic activity, which may have imposed intermittent environmental/ecological restrictions for the migrant taxa. An alternative model, more limited in extent considering the small areas involved and dependent upon past sea-level fluctuations, involves an eastward stepping stone-like route toward Chiloé Continental through the Chilotan archipelago (Fig. 1).

Fundamental questions, currently unaddressed by a virtual lack of studies in the Chiloé Continental region, include: 1) when did local ice-free conditions establish in the region? 2) when and what vegetation type colonized this sector during the early phases of T1? 3) is there geomorphic/stratigraphic evidence for the stabilization or readvances of Andean glaciers during T1? 4) is there evidence for climate reversals akin to the Antarctic Cold Reversal and/or the Younger Dryas? 5) when did forest vegetation establish in the study area? and 6) did physical/climatic/ecological barriers to dispersal cause a delay in the arrival of plant taxa into the Chiloé Continental region during T1 and the Holocene?

2. Methods

We obtained lake sediment cores from Lago Proschle (41°52.143′S, 72°46.675′W, 53 m.a.s.l., 460 cm water depth) (Fig. 1), using a 7.5-cm-diameter water-sediment interface piston corer and a 5-cm-diameter Wright piston corer from the deepest central sector of the lake. Sediment retrieval was conducted from an anchored coring rig equipped with a 7.5-cm diameter aluminum casing tube. All sediment cores were stored at 4 °C at the Quaternary Paleoecology Laboratory of Universidad de Chile, subsequently X-radiographed to document the stratigraphy and potential stratigraphic structures, and subsampled for loss-on-ignition (LOI, 1 cc), pollen (1 cc) and macroscopic charcoal (2 cc) analyses following standard protocols (Faegri and Iversen, 1989; Heiri et al., 2001; Whitlock and Anderson, 2003). The LOI results are expressed as percent weight loss (organic and carbonate percent: LOI_{550} and LOI_{925}, respectively) and dry siliciclastic density data (LOI_{925} ash).

The chronology of the sedimentary records is constrained by AMS radiocarbon dates obtained from bulk organic samples retrieved from 1-cm-thick sections throughout the cores. We calibrated the radiocarbon dates using the SHCal13 calibration dataset (Hogg et al., 2013) included in CALIB 7.0.0 (Reimer et al., 2013) and developed a Bayesian age model on the Lago Proschle dates using the Bacon package for R (Blaauw and Christen, 2011). The age model takes into account the instantaneous deposition of pyroclastic levels by subtracting the thickness of all tephra layers >1 cm.

I studied the palynology of the Lago Proschle cores following standard procedures for organic-rich lake sediments lacking carbonates. These results are shown in percentage diagrams and organized in life forms, habitat occurrence (arboreal, non-arboreal, aquatic, microscopic algae) and native/non-native. Identification of fossil palynomorphs was conducted at 400X magnification using a

ZEISS Axio Scope A1 stereomicroscope with the aid of published descriptions and keys (Heusser, 1971; Villagrán, 1980), along with a modern reference collection. The palynomorph *Fitzroya/Pilgerodendron* includes the species *Fitzroya cupressoides* and *Pilgerodendron uviferum,* mainly distributed in the Pacific coasts of Patagonia; *Nothofagus dombeyi* type, hereafter referred as *Nothofagus*, includes the species *N. dombeyi, N. nitida, N. betuloides, N. pumilio* and *N. antarctica,* present in northwestern Patagonia; *Eucryphia/Caldcluvia* includes the species *Eucryphia cordifolia* and *Caldcluvia paniculata; Lomatia/Gevuina the species Lomatia ferruginea, L. dentata, L. hirsuta,* and *Gevuina avellana; Maytenus disticha* type includes the species *M. disticha* and *M. magellanica.*

The terrestrial pollen sum (TPS) includes the pollen counts of arboreal and non-arboreal land plants; their percentage abundance is calculated in reference to the TPS. The aquatic pollen sum (APS) includes paludal plants, macrophytes and microalgae; their percentage abundance is expressed in reference to TPS + APS. We divided the pollen record in pollen assemblage zones with the aid of a stratigraphically constrained cluster analysis applied to all terrestrial taxa with abundance values $\geq$ 2%, after recalculating sums and percentages and converting to square root values using CONISS (Grimm, 1987) implemented in Tilia 2.0.38. The same subset of terrestrial taxa $\geq$2%, with recalculated sums and percentages, were smoothed with a moving average window applied to $\leq$5 and $\geq$ 3 adjacent pollen samples and interpolated every 100-year regular steps to allow calculation of the rates-of-change (ROC) parameter (Grimm and Jacobson, 1992; Jacobson et al., 1987). The squared chord distance is a dissimilarity coefficient quantifies the magnitude and rapidity of changes between adjacent samples in the pollen dataset, allowing examination of the abruptness or graduality of past shifts in the terrestrial vegetation. I standardized the ROC time series to the mean of the entire record to characterize values around the mean (>-1σ, < 1σ), rapid (>1σ, < 2σ), abrupt (>2σ, < 3σ), and extraordinarily fast vegetation changes (>3σ) in the pollen stratigraphy.

We tallied macroscopic charcoal particles (>106 mm) on the Lago Proschle cores from 2-cc sediment samples along continuous contiguous 1-cm thick sections throughout the cores under a Zeiss KL1500 LCD stereoscope, following careful sieving to avoid rupture of individual particles. The abundance of macroscopic charcoal is expressed as accumulation rate data (particles*cm^{-2}*year^{-1}). I applied a time-series analysis tool, CharAnalysis (Higuera et al., 2009), to the charcoal record to detect statistically significant charcoal peaks from the low-frequency background signal and deconvolute a local fire history. For that purpose I interpolated the macroscopic charcoal record to the median time step between adjacent samples and defined background charcoal with a lowess robust to outliers and a smoothing window of 1000 years. The peaks component corresponds to the 99th percentile distribution of positive residuals using a locally defined threshold. I calculated the frequency of fire events per 1000 year overlapping time windows and charcoal peak magnitude.

3. Results

I combined cores 0505SC1, 0505BT1 and the 0505CT1-CT4 series to produce a continuous sedimentary record (Fig. 2) that spans from the onset of lacustrine sedimentation in Lago Proschle until the present. The spliced record has a total length of 472 cm and consists of a fining upward basal sand/gravel unit between 472 and 460 cm depth, overlain by a fining upward sandy silt unit with increasing amount of organic material that persists until it reaches a maximum of ~70% organic matter at 333 cm depth (Fig. 2). This organic-rich silty unit is capped by an 18-cm thick tephra, which gives way to an organic-poor silty unit, whose organic content increases steadily until it reaches a maximum of ~80% at 110-109 cm depth. Within the latter I detect discrete clastic peaks at 280–279, 243–242, 236–235, 168–164, and 159-158 cm depth I interpret as tephra layers. The upper portion of the record features a decline in the organic content of the organic-rich silts following deposition of tephra at 110–109, 88–93 and 80-79 cm depth (Fig. 2).

The chronology of the Lago Proschle record is constrained by 22 AMS radiocarbon dates on bulk organic lake sediment. These data indicate continuous sedimentation of organic-rich lake sediments since the beginning of lacustrine deposition at ~17.4 ka (Fig. 3, Table 1). The pollen record from Lago Proschle consists of 411 samples that span continuously the last ~17,400 years with a median temporal resolution of 38 years between palynological samples. I divided the record in 9 pollen zones with the aid of a stratigraphically constrained cluster analysis to facilitate description of the major changes in the pollen record (Fig. 4). In the following paragraphs I describe each zone highlighting the three most abundant taxa in decreasing order of mean abundance, their cumulative abundance in relation to the terrestrial pollen sum, the mean arboreal pollen percentage of the zone, their accompanying less-abundant taxa, the average percent abundance of any given taxon in parenthesis, and remarks about the most conspicuous changes of each zone (see Table 2).

Zone Pro-1 (19 samples, 453-423 cm depth, ~17.4–16.3 ka) features the pollen assemblage *Nothofagus*-Poaceae-*Empetrum*, which accounts for 75.2% of the Terrestrial Pollen (TP) sum. The dominant taxa achieve their maximum abundance of the entire record during this zone, accompanied by peak abundance of *Maytenus disticha* type (2.9%), the fern *Blechnum* type (42.4%), along with the aquatic Cyperaceae (5%) and the microalga *Pediastrum* (max: 20.3%). Other trees and shrubs are present in relatively small abundance (*Fitzroya/Pilgerodendron*: 1.6%, *Escallonia*: 2.8%, Myrtaceae: 2.6%) including *Drimys*, which rises and achieves relatively high abundance (3.2%) toward the end of this zone. *Misodendrum* shows a modest maximum during intermediate *Nothofagus* levels (~50%). The mean arboreal pollen (AP) sum is 74.9%, and constitutes the lowest value in the entire record.

Zone Pro-2 (14 samples, 423-407 cm depth, ~16.3–15.4 ka) is characterized by the assemblage *Nothofagus*-Myrtaceae-Poaceae (79% of TP, AP: 92%), along with declines in Poaceae (from 11.5% to 4.4%), *Empetrum* (from 8.8% to 2%), *Blechnum* type (from 42.4% to 17.9%), and Cyperaceae (5%–2.5%). Myrtaceae increases rapidly to its peak abundance (max: 38.6%) as *Nothofagus* undergoes large-magnitude oscillations. *Drimys winteri* (3.5%) and *Escallonia* (2.8%) attain their maximum abundance. *Lomatia/Gevuina* appears in the record and remains in low abundance (<3%) in the entire record. Cyperaceae declines during this zone and reaches its lowest abundance during the next zone.

Zone Pro-3 (31 samples, 407-373 cm depth, ~15.4–13.5 ka) is dominated by *Nothofagus*, *Podocarpus nubigena* and Myrtaceae (72.7% of TP, AP: 97.4%), resulting from a major decline in Myrtaceae (from 28.3% to 8%) and a virtual disappearance of Poaceae, *Empetrum, Maytenus disticha* type, *Blechnum* type and *Drimys*. *P. nubigena* rises rapidly to its peak abundance (max: 46.2%), contemporaneous with a rise in *Raukaua* to its maximum in the record (2%), while *Fitzroya/Pilgerodendron* shows a slight increase (2.9%) that culminates in the next pollen zone. *Misodendrum* shows a modest maximum during intermediate *Nothofagus* levels (~50%). Cyperaceae attains minimum abundance during this zone (<1%).

Zone Pro-4 (17 samples, 373-356 cm depth, ~13.5–12.6 ka) features the assemblage *Nothofagus-Podocarpus nubigena-Tepualia stipularis* (79% of TP, AP: 96.6%). Noteworthly aspects of this zone are a decline in *P. nubigena* (from 29.6% to 23.5%), large-magnitude oscillations in *Nothofagus,* and a conspicuous increase in *T. stipularis*

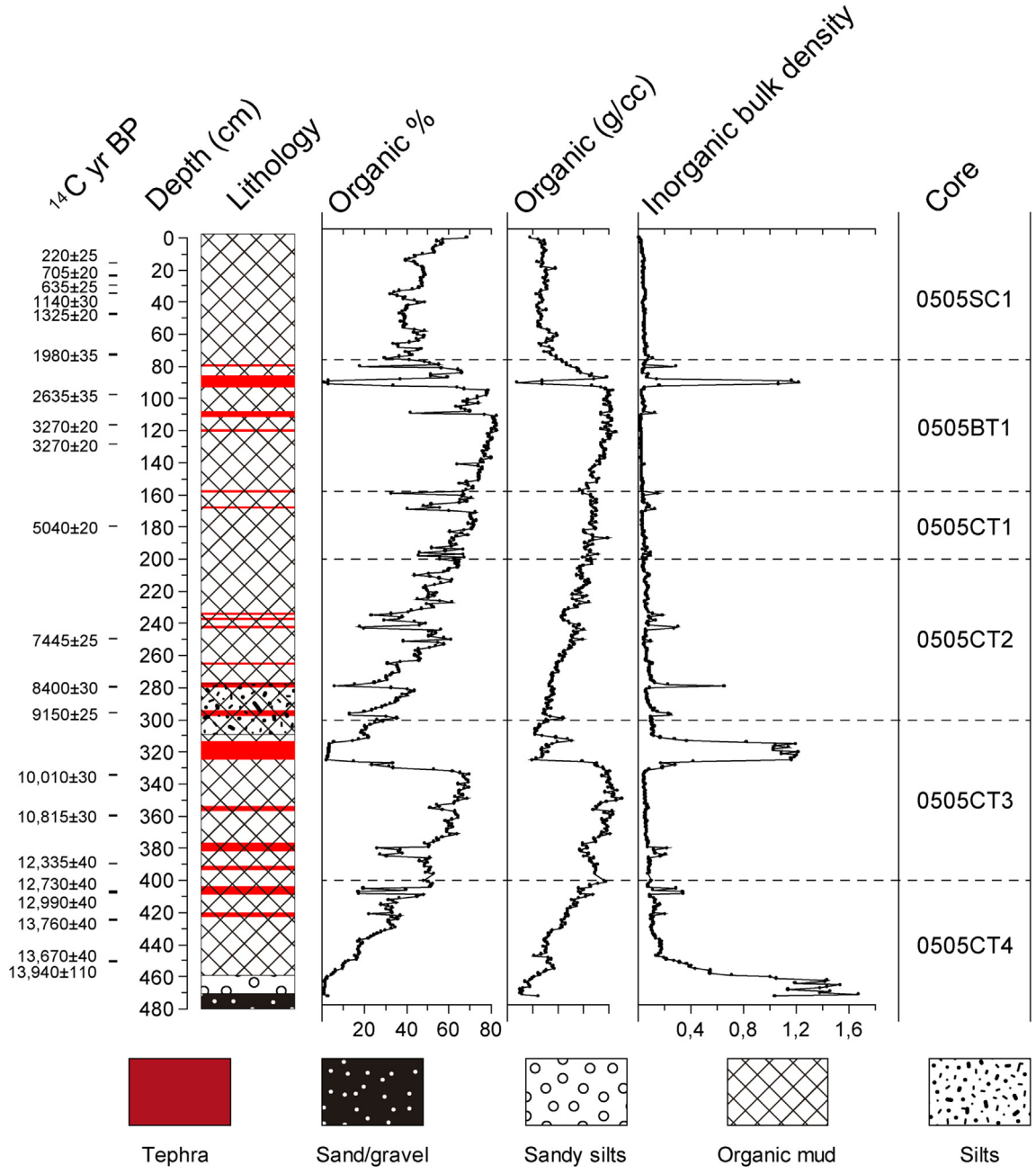

Fig. 2. Stratigraphic column, radiocarbon dates, and loss-on-ignition data from the Lago Proschle site. The labels on the left show the stratigraphic position and age of radiocarbon-dated levels, in some instances the radiocarbon date labels were displaced vertically to facilitate visualization of the ages. The labels on the right indicate the identity and stratigraphic span (dashed horizontal lines) of each core segment.

(from <1% to 8.2%). *Fitzroya/Pilgerodendron* culminates a rising trend at the end of this zone (max: 6.8%). *Misodendrum* shows a modest maximum during intermediate *Nothofagus* levels (~50%).

Zone Pro-5 (46 samples, 356-295 cm depth, ~12.6–10.3 ka) represents the largest change in the record, according to the stratigraphically constrained cluster analysis, and consists of a *Weinmannia trichosperma-Tepualia stipularis-Nothofagus* assemblage (63% of TP, AP: 91.5%). I observe a rapid rise in *W. trichosperma* (from 2.4% to 39.9%) and substantial declines in *P. nubigena* (from 23.5% to 3.8%) and *Nothofagus* (from 41% to 11.3%) relative to Pro-4. *T. stipularis* (11.8%) and *Hydrangea* (4.7%, max: 11.5%) attain their maximum abundance and *Fitzroya/Pilgerodendron* initiates a gradual declining trend. *Eucryphia/Caldcluvia* appears in the record with values consistently below 5% prior to ~11.2 ka, and larger variability (between 0 and 15%) thereafter.

Zone Pro-6 (30 samples, 295-265 cm depth, ~10.3–8.9 ka) is dominated by an *Eucryphia/Caldcluvia-Nothofagus-Weinmannia trichosperma* pollen assemblage (63% of TP, AP: 93.5%). *Eucryphia/Caldcluvia* rose rapidly (from 2.6% to 34.6%, max: 54%) accompanied by a gradual and sustained increase in *Nothofagus* (from 11.3% to 14.6%) and substantial declines in *W. trichosperma* (from 40% to 13.1%) relative to Pro-5.

Zone Pro-7 (30 samples, 265-235 cm depth, ~8.9–7.8 ka) is characterized by a *Nothofagus-Eucryphia/Caldcluvia*-Myrtaceae assemblage (62.1% of TP, AP: 93.5%), resulting from a rise in *Nothofagus* (from 14.6% to 33.8%) and decreasing abundance of

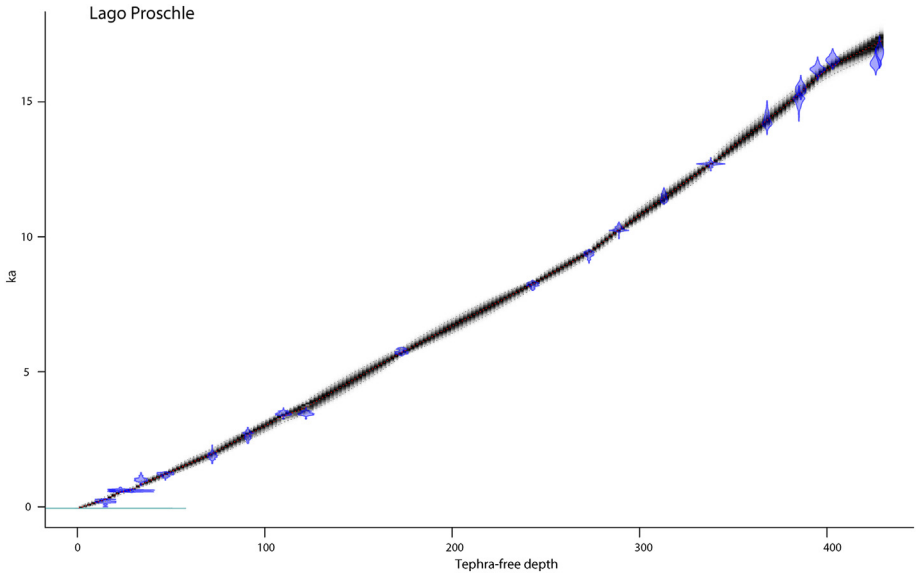

Fig. 3. Age model of the Lago Proschle site using a tephra-free depth scale. The blue zones represent the probability distribution of the calibrated radiocarbon dates, the grey zone represents the calculated confidence interval (95.4%) of the Bayesian age model. (For interpretation of the references to color in this figure legend, the reader is referred to the Web version of this article.)

Table 1
Radiocarbon dates from the Lago Proschle site. The radiocarbon dates were calibrated to calendar years before present using the CALIB 7.0 program.

Laboratory code	Core code and length	Original depth (cm)	Tephra-free depth (cm)	^{14}C yr BP	1 sigma error	lower intercept (cal yr BP)	upper intercept (cal yr BP)	median probability (cal yr BP)
uciams-145167	0505SC_15	15	15	220	25	75	300	195
uciams-122760	0505SC_23	23	23	705	20	563	664	599
uciams-145168	0505SC_29	29	29	635	20	545	634	608
cams-128986	0505SC_34	34	34	1140	60	910	1178	1007
uciams-122761	0505SC_47	47	47	1325	20	1179	1273	1228
cams-128987	050AT1_36	72	72	1980	70	1715	2045	1887
uciams-128988	0505BT1_30	96	91	2635	70	2437	2855	2687
uciams-122762	0505BT1_49	115	110	3270	20	3379	3556	3443
uciams-122763	0505BT1_61	127	122	3270	20	3379	3556	3443
uciams-122764	0505CT1_79	178	173	5040	20	5648	5887	5721
uciams-122765	0505CT2_47	248	243	7445	25	8171	8327	8250
uciams-122766	0505CT2_77	278	273	8400	30	9289	9470	9384
uciams-122767	0505CT2_93	294	289	9150	25	10201	10374	10247
uciams-122768	0505CT3_32	336	313	10010	30	11260	11607	11383
uciams-122769	0505CT3_57	361	338	10815	30	12674	12737	12704
uciams-122770	0505CT3_87	391	368	12335	40	14043	14538	14218
uciams-122771	0505CT4_7	408	385	12730	40	14878	15284	15115
cams-114967	0505DT4_958	409	386	12990	80	15210	15763	15479
uciams-145962	0505CT4_17	418	395	13510	60	15981	16454	16206
uciams-122772	0505CT4_25	426	403	13760	40	16328	16807	16556
cams-114966	0505CT4_1003	449	426	13670	80	16166	16754	16429
uciams-145169	0505CT4_50	451	428	13940	110	16432	17202	16836

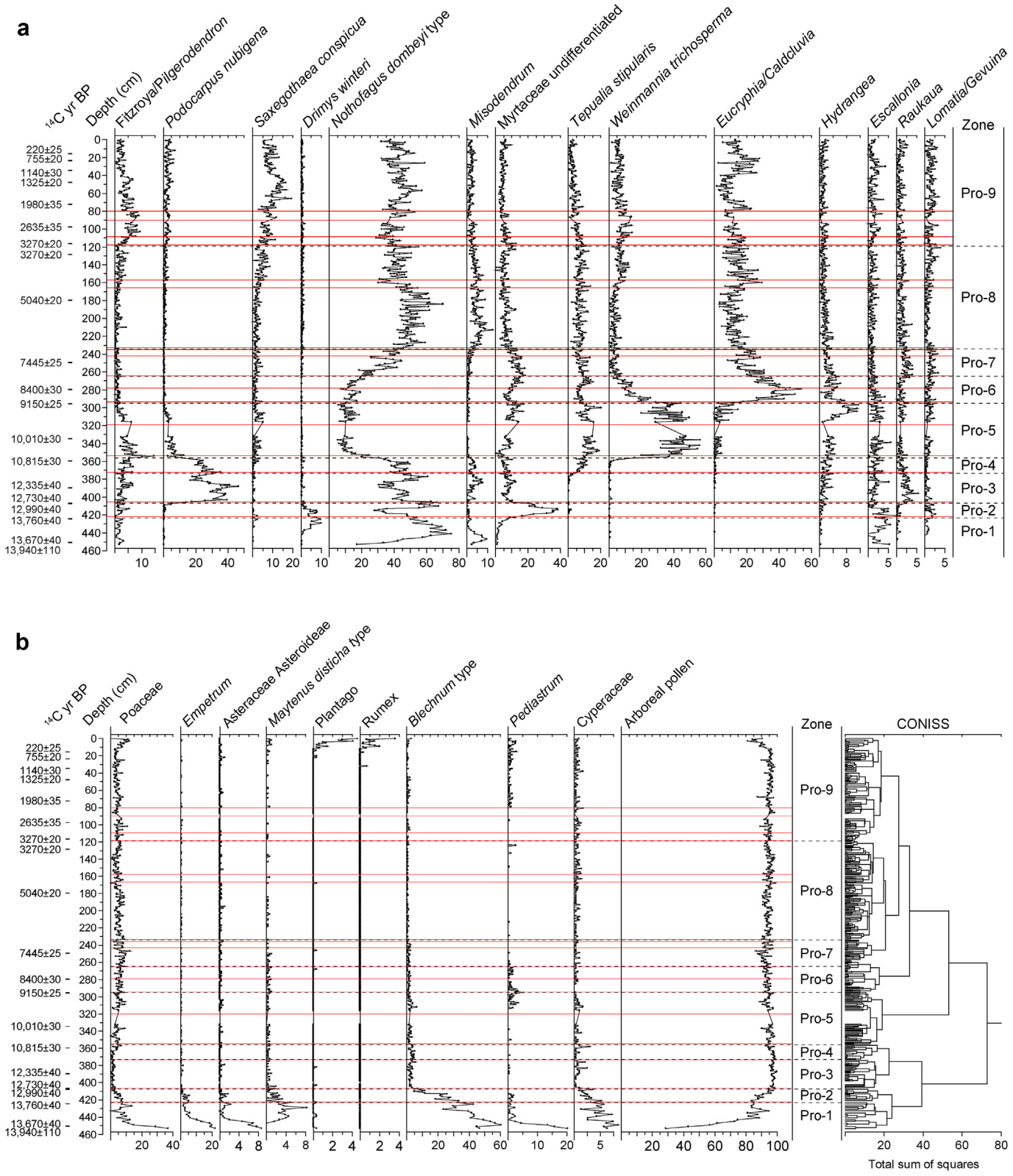

Fig. 4. Percentage pollen diagram from the Lago Proschle site. The labels on the left show the stratigraphic position and age of radiocarbon-dated levels used in the age model. The labels on the right indicate the identity and stratigraphic span (black dashed horizontal lines) of each pollen assemblage zone. The horizontal red lines indicate the stratigraphic position of tephra layers. (For interpretation of the references to color in this figure legend, the reader is referred to the Web version of this article.)

Table 2
Summary of the pollen assemblage zones from the Lago Proschle record specifying the three most abundant taxa in decreasing order of mean abundance along, their cumulative abundance in parentheses, stratigraphic and chronologic range, and number of levels analyzed per zone.

Zone	Depth range (cm)	Number of samples	Age range (ka)	Pollen assemblage	TP sum	AP sum
Pro-1	453–423	19	~17.4–16.3	*Nothofagus*-Poaceae-*Empetrum*	75.2%	74.9%
Pro-2	423–407	14	~16.3–15.4	*Nothofagus*-Myrtaceae-Poaceae	79%	92%
Pro-3	407–373	31	~15.4–13.5	*Nothofagus-Podocarpus nubigena*-Myrtaceae	72.7%	97.4%
Pro-4	373–356	17	~13.5–12.6	*Nothofagus-Podocarpus nubigena-Tepualia stipularis*	79%	96.6%
Pro-5	356–295	46	~12.6–10.3	*Weinmannia trichosperma-Tepualia stipularis-Nothofagus*	63%	91.5%
Pro-6	295–265	30	~10.3–8.9	*Eucryphia/Caldcluvia-Nothofagus-Weinmannia trichosperma*	63%	93.5%
Pro-7	265–235	30	~8.9–7.8	*Nothofagus-Eucryphia/Caldcluvia*-Myrtaceae	62.1%	93.5%
Pro-8	235–119	115	~7.8–3.5	*Nothofagus-Eucryphia/Caldcluvia-Tepualia stipularis*	67.2%	94.4%
Pro-9	119–0	112	~3.5 ka- present	*Nothofagus-Eucryphia/Caldcluvia-Saxegothaea conspicua*	63.4%	94.4%

Eucryphia/Caldcluvia (from 34.6% to 20.4%).

Zone Pro-8 (115 samples, 235-119 cm depth, ~7.8–3.5 ka) features dominance of *Nothofagus*, *Eucryphia/Caldcluvia*, and *Tepualia stipularis* (67.2% of TP, AP: 94.4%), accompanied by Myrtaceae (6.2%), peak abundance of *Nothofagus* (from 33.8% to 46.9%), coeval with gradual increases in *Saxegothaea conspicua* and *Weinmannia trichosperma*, and a decline in *Eucryphia/Caldcluvia* (from 20.4% to 13.3%). *Misodendrum* shows a gradual increase to a maximum of 12.5% during a *Nothofagus* plateau of ~50% and declines gradually toward the end of this zone. We observe centennial-scale oscillations in antiphase between *Nothofagus* type and *Eucryphia/Caldcluvia* starting near the middle of this zone (~6 ka)

Zone Pro-9 (112 samples, 119-0 cm depth, ~3.5 ka-present) is characterized by a *Nothofagus-Eucryphia/Caldcluvia-Saxegothaea conspicua* assemblage (63.4% of TP, AP: 94.4%), and features culmination of the rising trends in *S. conspicua* (from 2.9% to 9.1%) and *W. trichosperma* (from 4.9% to 6.9%).

The rates-of-change analysis (Fig. 5) applied to the pollen record reveals high values between ~17.4 and ~15.3 ka, falling in the range of rapid and abrupt changes, followed by predominantly low values around the mean for the remainder of the record. A major increase peaked at ~12.7 ka, defining an extraordinarily fast vegetation change, superseded by discrete peaks at ~10.3, ~8.2, ~5.3, ~2.6, ~1.8, ~1.1, ~0.6 ka, and during the 20th century. The majority of these correspond to rapid changes, the peaks at ~1.8 ka and during the 20th century qualify as abrupt changes.

The continuous-contiguous macroscopic charcoal record of Lago Proschle (Fig. 6) includes 429 levels that span continuously the last ~17,400 years, with a median temporal resolution of 38 years. The record shows very low values between ~17.4 and ~13 ka punctuated by discrete increments; this interval is followed by a major rise with multiple large-magnitude maxima between ~13 and ~11 ka, and intermediate values between ~10 and ~9.5 ka. Another rise is evident between ~9 and ~7.8 ka, followed by persistently low values over the last ~7000 years with a discrete rise at ~4.3 ka. Time series analysis of the macroscopic charcoal data (Fig. 6) reveals 32 statistically significant charcoal peaks, most of which exhibit low magnitudes (<40 particles*cm^{-2}*yr^{-1}). A conspicuous clustering of events is evident between ~14.7 and ~11.3 ka with large-magnitude events dated at ~12.8 and ~4.3 ka. Fire frequency shows a mean of 1.8 events/1000 yr, with distinct millennial-scale variations that include maximum frequency at ~16 and ~5.5 ka, and minimum values at ~3.5 ka.

4. Discussion

4.1. Paleovegetation inferences

The pollen record from Lago Proschle starts with a brief pioneer phase dominated by herbs and shrubs (Poaceae, *Empetrum*, Asteraceae subfamily Asteroidae, *Maytenus disticha* type) (Figs. 4 and 5) typically found in the modern High Andean environments of northwestern Patagonia, suggesting colonization of the barren, newly deglaciated landscapes of the western Andean foothills by cold-tolerant plants during the earliest stages of T1. Ferns of the genus *Blechnum*, possibly *B. penna-marina*, were particularly abundant prior to ~17 ka suggesting low arboreal cover and overall humid conditions. Though modest in magnitude, the macrophyte Cyperaceae attained the maximum abundance of the entire record prior to ~16 ka, accompanied by peak percentages of the microalga *Pediastrum* during the initial 400 years of the record. The terrestrial vegetation then shifted to temperate forests as *Nothofagus* rose ~60% between ~17.4 and ~17 ka, indicating a rapid spread of cold-tolerant, shade-intolerant, opportunistic trees. This was concomitant with a steady decrease of *Blechnum* type and the rise, peak, and decline of *Drimys*, a shade-intolerant tree species (Figueroa and Lusk, 2001) that commonly dominates large forest gaps following disturbance, thus accounting for the initial phases of a woodland encroachment process. This transition toward a forested landscape is captured by the rates-of-change (ROC) parameter as an abrupt vegetation change (Fig. 5). A subsequent rise in the shade tolerant and thermophilous Myrtaceae at ~16.3 ka (2σ confidence interval [CI]: 16.6–16 ka) marks the establishment of closed-canopy North Patagonian Rain Forests (NPRF). Several genera and species of the family Myrtaceae are abundant in VRF and NPRF communities located in lowland sectors (<400 m.a.s.l.) of northwestern Patagonia (*Amomyrtus luma, A. meli, Blepharocalyx cruckshanksii, Luma apiculata, Myrceugenia chrysocarpa, M. ovata, M. parvilora, M. planipes, Tepualia stipularis, Ugni molinae,* etc.), both in upland and waterlogged environments (Heusser et al., 1999; Villagrán, 1985). A marked decline in the abundance of Myrtaceae at higher elevations (400–700 m.a.s.l.) revealed by modern vegetation surveys (Villagrán, 1985), suggests that low temperatures constitute a limiting factor for their occurrence in montane evergreen rainforests. Consequently, I interpret the Myrtaceae rise at ~16.3 ka as indicative of warmer and wetter conditions than the preceding millennium. This vegetation change coincided with a persistent decline in fire frequency, which had risen steadily between ~17 and ~16 ka (Fig. 6), and decreased abundance of Cyperaceae between ~16.3 and ~15.4 ka (Figs. 4 and 7). I interpret the latter as a lake-level rise which drove an outward shift of littoral environments away from the deepest sector of the lake, where the coring site is located. Consequently, I infer a major environmental transformation that led to the establishment of closed-canopy NPRF, a decline in fire activity, and a transgressive lacustrine phase in Lago Proschle starting at ~16.3 ka (Figs. 4–6).

Podocarpus nubigena and *Raukaua* rose at ~15.4 ka (2σ CI: 15.7–15.2 ka) and attained their maxima between ~15 and ~12.8 ka, along with *Tepualia stipularis, Hydrangea*, *Saxegothaea conspicua* and *Fitzroya/Pilgerodendron* (Figs. 4 and 5). This change suggests a vegetation shift toward closed-canopy NPRF dominated by *Nothofagus*, cold-tolerant conifers, and hygrophilous trees, while fire

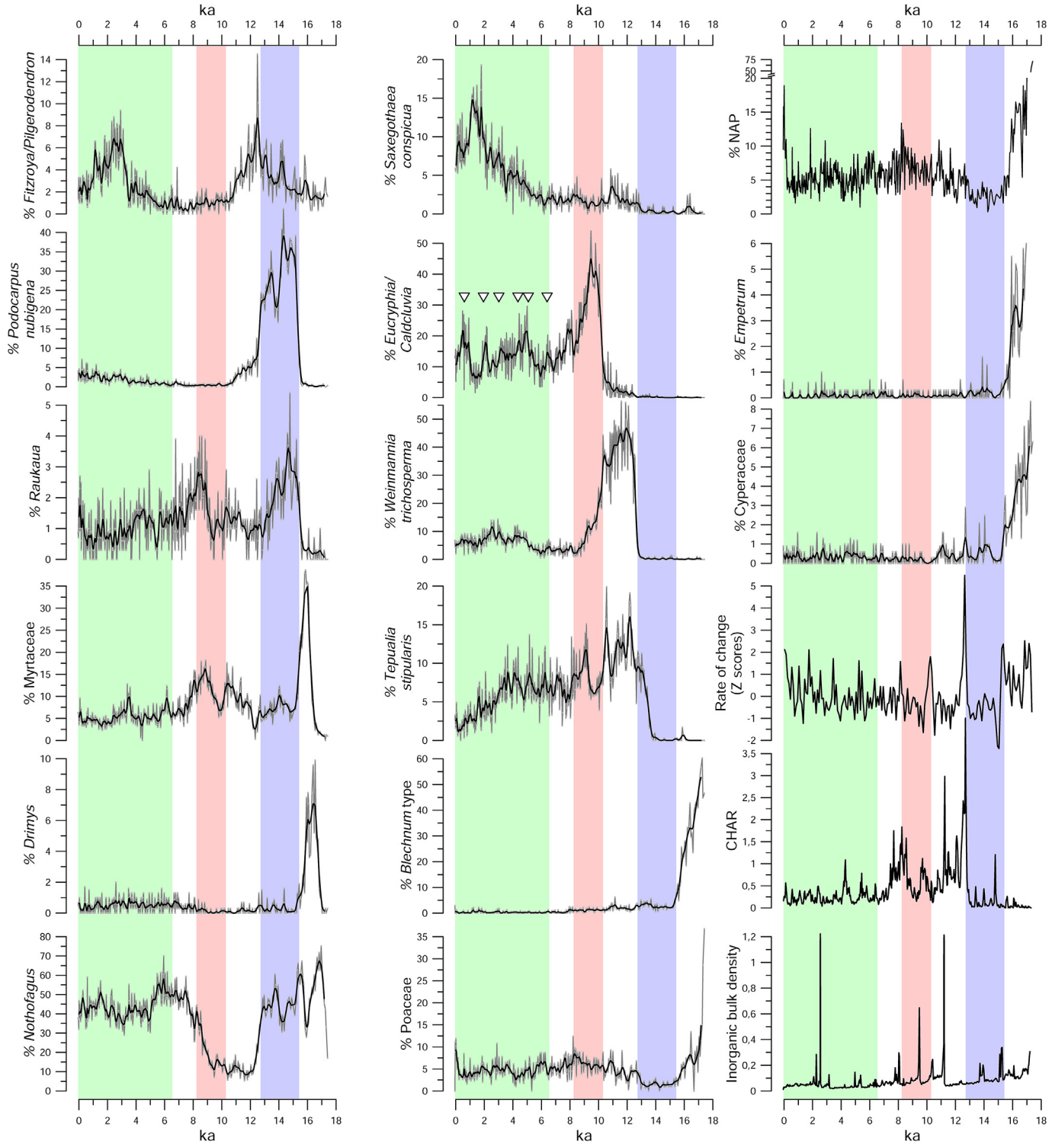

Fig. 5. Selected variables from the Lago Proschle pollen record shown in the time scale domain. Each time series is shown with a weighted running mean of seven adjacent samples with a triangular filter. The vertical colored ribbons highlight selected intervals characterized by multi-millennial shifts to cold/wet (blue) and warm/dry (red), conditions, along with a multi-millennial Holocene interval featuring alternations between warm/dry and cold/wet phases at centennial timescales (green). The white triangles highlight the centennial-scale increments in *Eucryphia/Caldcluvia* discussed in the main text. Also shown are the calculated rates-of-change (ROC) parameter in the far right, the Macroscopic Charcoal Accumulation Rate (CHAR), and the siliciclastic density data. (For interpretation of the references to color in this figure legend, the reader is referred to the Web version of this article.)

activity remained low with discrete low-magnitude events (Figs. 5 and 6). The ROC value for this transition falls in the range of abrupt vegetation changes (Figs. 5 and 6). An increase in *Weinmannia trichosperma* from <2% to >50% occurred between ~12.8 ka (2σ CI: 13–12.6 ka) and ~12 ka (2σ CI: 12.3–11.9 ka), accompanied by declines in *Podocarpus nubigena* and *Nothofagus*, persistence of

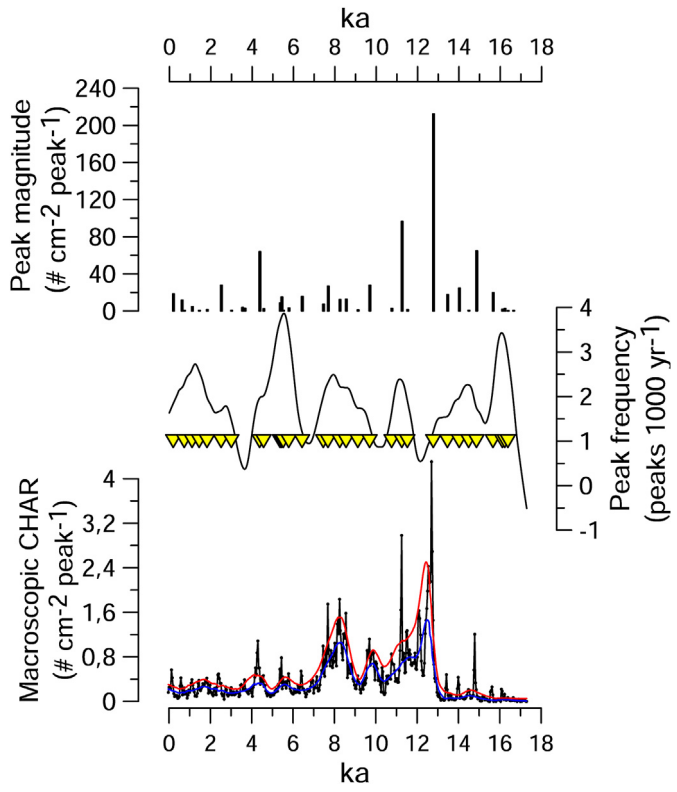

Fig. 6. Macroscopic charcoal record from the Lago Proschle site and results of CharAnalysis: blue line: background component, red line: locally defined threshold, triangles: statistically significant charcoal peaks, magnitude: residual abundance that supersedes the threshold. (For interpretation of the references to color in this figure legend, the reader is referred to the Web version of this article.)

Tepualia stipularis, modest increases in *Eucryphia/Caldcluvia*, Myrtaceae and Poaceae (Figs. 4 and 5), and a major increment in CHAR (Fig. 6). These results suggest opening of the forest canopy by wildfires, substantial declines in shade- and cold-tolerant NPRF conifers, and proliferation of shade-intolerant trees favored by disturbance. The character, magnitude, and rapidity of palynological changes suggests the occurrence of stand-replacing fires, i.e. local fires that kill all or most of the living overstory trees, initiate forest succession, and cause a sudden species turnover. This event is captured by the ROC parameter as an extraordinarily fast vegetation change, the highest in the entire record (Fig. 5). This remarkable change was contemporaneous with the largest-magnitude increase in Charcoal Accumulation Rates (Figs. 5 and 6), suggesting that fire disturbance acted as a catalyst or amplifier of climate-driven changes in vegetation.

The vine *Hydrangea* increased between ~11.2 and ~10.3 ka, followed by a rapid ~50% rise in *Eucryphia/Caldcluvia* between ~10.3 and ~9.5 ka, and declines in most trees (Figs. 4 and 5). The palynomorph *Eucryphia/Caldcluvia* includes the species *Eucryphia cordifolia* which is an endemic tree of the evergreen temperate forests of southern South America, and today occurs exclusively in Valdivian Rainforest (VRF) communities. Hence, the palynologic signal that started at ~10.3 ka (2σ CI: 10.5–10.2 ka) (Figs. 4 and 5) marks an important vegetation change from North Patagonian to Valdivian-dominated rainforests. This was a rapid transition according to the ROC parameter, one of the highest peaks during the Holocene (Fig. 5). Vegetation change was accompanied by a fire-regime shift consisting of frequent local fire events of intermediate magnitude (Figs. 5 and 6), suggesting that fire disturbance acted as a catalyst or amplifier of climate-driven changes in the local vegetation. *Eucryphia cordifolia* then declined from ~9.5 to ~7.8 ka, punctuated by a short-lived increase between ~8.1 and ~7.8 ka associated with enhanced fire activity, a ~40% rise in *Nothofagus*, and culmination of a moderate Poaceae rise (Figs. 4–6). The latter increases may represent a response of the local vegetation to disturbance by fire, considering that several species of the genus *Nothofagus* have been reported as fast-growth, pioneer, and opportunistic trees in disturbed terrains, and species of the native bamboo genus *Chusquea* (which belongs to the Poaceae family) commonly form dense thickets in forest gaps and woodland edges.

A steady increase in *Nothofagus* led to a maximum between ~7.8 and ~5.4 ka contemporaneous with sustained increments in *Podocarpus nubigena, Saxegothaea conspicua* and *Drimys,* low abundance of *Weinmannia trichosperma* and *Eucryphia/Caldcluvia* (Figs. 4 and 5), and a declining trend in CHAR (Fig. 6). This assemblage indicates dominance of closed-canopy evergreen temperate rainforests, in the context of which the *Nothofagus* palynological signal most likely represents the species *N. dombeyi* and/or *N. nitida*. The co-occurrence of indicator species belonging to the VRF and NPRF suggests intermingling of these communities in the Andean foothills of northwestern Patagonia in the context of diminished fire activity. The ROC values associated with the transition toward a mixed NPRF-VRF assemblage suggests this was a gradual change (Fig. 5).

The most recent ~5400 years of the Lago Proschle record feature: (i) a continuation of the *Podocarpus nubigena* and *Saxegothaea conspicua* rising trends; (ii) a conspicuous increase in *Fitzroya/Pilgerodendron* at ~3.5 ka that reached a maximum between ~3 and ~2.5 ka and declined toward the present with short-lived fluctuations; (iii) a *Nothofagus* plateau at ~40% with recurrent increases until the present; along with (iv) an increase in *Weinmannia trichosperma* that peaked at ~2.5 ka overprinted by centennial-scale fluctuations, and (v) centennial-scale increases in *Eucryphia/Caldcluvia* with maxima at ~5, ~4.5, ~3.2, ~2.1, ~1, and ~0.4 ka (Figs. 4 and 5). A precursory centennial-scale increase in *Eucryphia/Caldcluvia* is also evident at ~6.4 ka, just before the final *Nothofagus* increase that led to its maximum Holocene abundance between ~6 and ~5.4 ka. These alternations suggest reshuffling and variations in the relative dominance of NPRF and VRF elements at timescales ranging from centennial to millennial. These floristic elements were already present in the lowlands of northwestern Patagonia during that portion of the Holocene, and their variations occurred in the context of low frequency changes of small to intermediate-magnitude fire episodes. The vegetation changes associated with these transitions were rapid (Fig. 5).

I observe increases in Poaceae, *Rumex* and *Plantago* starting at ~166 cal yr BP (2σ CI: 253-86 cal yr BP) following a fire episode at ~188 cal yr BP (2σ CI: 277-106 cal yr BP) (Figs. 4–6). Although these pollen taxa include native and exotic species, the observed increases (>3%) exceed their typical abundance throughout the entire Lago Proschle record (<1%). The Non Arboreal Pollen sum attained values permanently above the natural variability since the local establishment of closed-canopy temperate rainforests (~16.3 ka) (Figs. 4 and 5), and achieved a maximum of 19% during the 20th century, approximately twice the recorded values since ~15.8 ka. I interpret these changes as indicative of disturbance by Chilean/Europeans settlers during the most recent centuries by means of fire, and subsequent spread of non-native plant species (*Rumex acetosella* and *Plantago lanceolata*). The dominance of temperate evergreen rainforests persisted over the last three centuries, despite the unprecedented magnitude of human-induced disturbance recorded over the last century (Figs. 4 and 5).

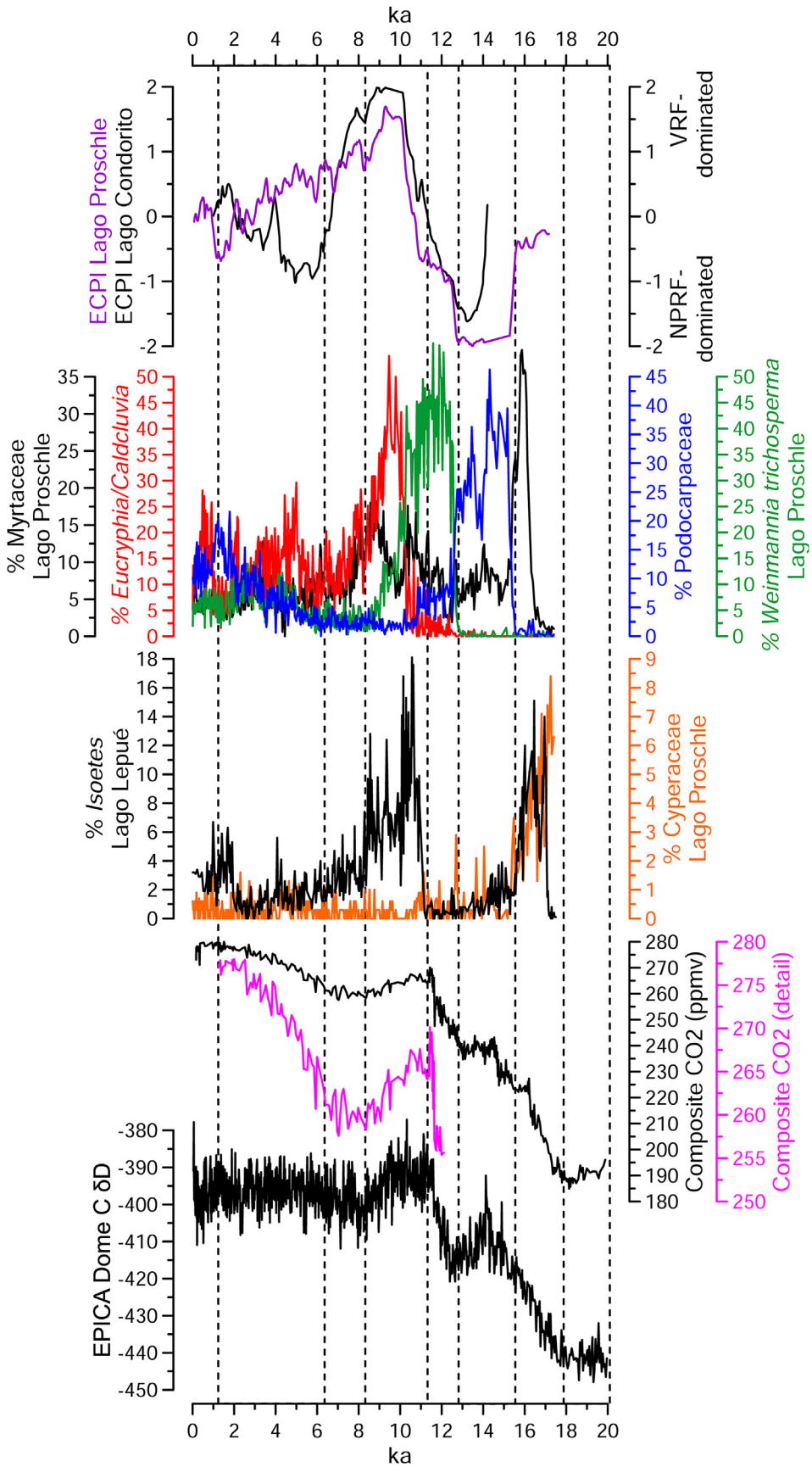

Fig. 7. Comparison of selected pollen taxa and Charcoal Accumulation Rates (CHAR) from Lago Proschle with palynological records from northwestern Patagonia (upper panel: the normalized ECPI [*Eucryphia/Caldcluvia* to Podocarpaceae pollen index] records from Lago Condorito (green curve) and L. El Salto (magenta curve), and the % *Isoetes* record from L. Lepué (red curve)), the Deuterium record from EDC and (lower panel) and a compilation of atmospheric CO_2 records from Antarctic ice cores (Bereiter et al., 2015). (For interpretation of the references to color in this figure legend, the reader is referred to the Web version of this article.)

4.2. Paleoclimate inferences

The Lago Proschle record spans continuously from ~17.4 ka (2σ CI: 17.9–17 ka) to the present. Lacustrine sedimentation in this site started after the Seno Reloncaví piedmont glacier lobe abandoned its final LGM moraines that rim the southernmost portion of the Longitudinal Valley, in the Puerto Montt area, and retreated ~40 km along the >300-m deep Seno Relocanví seaway (Rodrigo, 2006a, 2006b). Vegetation development led to the dominance of temperate rainforests near the study site, which have undergone compositional and structural changes that range from NPRF with abundant cold-tolerant hygrophilous conifers (*Fitzroya cupressoides, Pilgerodendron uviferum, Podocarpus nubigena, Saxegothaea conspicua*) during the final portion of T1, to assemblages with abundant thermophilous VRF tree species (*Eucryphia cordifolia*) tolerant to summer moisture deficit during the early Holocene. Transitions between these end members imply shifts in temperature and (annual, seasonal) precipitation, ranging from temperate-wet with little rainfall seasonality to warm-wet with strong rainfall seasonality, respectively. An intermediate or average condition is implied by pollen assemblages dominated by rainforest trees, vines, and ferns, lacking both cold-tolerant NPRF hygrophilous conifers and thermophilous VRF tree species tolerant to summer moisture deficit.

The palynology of Lago Proschle suggests that glacier recession into the high Andean cirques of northwestern Patagonia during T1 was contemporaneous with a warming trend coupled with low lake levels and fires between ~17.4 and ~16.3 ka. This low precipitation regime contrasts with the reconstructed cold and hyperhumid conditions during the final portion of the LGM (Heusser et al., 1995; Heusser et al., 1999; Heusser et al., 1996a, b; Moreno, 1997; Moreno et al., 2015; Moreno et al., 1999; Moreno et al., 2018a; Villagrán, 1985, 1988a, b, 1990), suggesting a transition from stronger-than-present to lower-than-present Southern Westerly Wind (SWW) influence at ~42°S (Moreno et al., 2018a). I interpret this transition as a poleward shift of the SWW at the beginning of T1. A subsequent establishment of Myrtaceae forests, lake level rise, and decline in fires after ~16.3 ka attests to a rise in precipitation at ~42°S. This transition suggests a northward shift of the SWW following the millennial-scale southward displacement discussed above.

Sustained warming culminated with the rapid establishment of evergreen, temperate, closed-canopy forests with thermophilous NPRF tree species between ~17.4 and ~15.4 ka and low abundance of cold-tolerant conifers near Lago Proschle, suggesting that vegetation near the site approached average Holocene conditions at that time. An abrupt shift toward cold/wet conditions ensued, implied by the dominance of *Nothofagus* (possibly *N. pumilio* or *N. betuloides*), cold-tolerant hygrophilous conifers (*Fitzroya cupressoides* or *Pilgerodendron uviferum*), and absence of fires between ~15.4 and ~12.8 ka. This abrupt transition suggests increased SWW influence in the region, probably representing a northward shift or intensification of this wind belt. A reversal in trend started at ~12.8 ka with proliferation of shade-intolerant trees favored by disturbance (*Weinmannia trichosperma*), a rise in CHAR suggesting intense local fire activity, and substantial declines in shade- and cold-tolerant NPRF conifers. These results indicate conditions favorable for biomass desiccation, stand-replacing fires, and disappearance of moisture-demanding shade-tolerant trees. The character and extraordinarily fast shift of this transition points to a sudden decline in summer precipitation and warmer summers, which in this region are linked to reduced SWW influence and cloudiness. Thermophilous, shade-intolerant, summer-drought tolerant VRF trees (*Eucryphia/Caldcluvia*) rose rapidly at ~10.3 ka and achieved their maximum abundance at ~9.5 ka in the context of high fire activity. *Nothofagus* and Poaceae increased between ~9.5 and ~7.8 ka, coeval with a gradual *Eucryphia/Caldcluvia* decline and a prominent increase in CHAR, suggesting local vegetation disturbance by fire. I interpret peak warmth and decline in annual precipitation brought by enhanced rainfall seasonality during the early Holocene (~10.3–7.8 ka). These results define a conspicuous warm interval with minimum SWW influence and maximum fire activity.

Nothofagus rose rapidly and attained its maximum Holocene abundance between ~6 and ~5.4 ka, along with increases in cold-tolerant/hygrophilous NPRF conifers, declines in *Weinmannia trichosperma*, the thermophilous/summer-drought tolerant VRF trees *Eucryphia/Caldcluvia*, and diminished fire activity. These data suggest a shift toward cooler/wetter conditions starting at ~7.8 ka, most likely related to enhanced SWW influence at ~42°S (Moreno and Videla, 2016; Pesce and Moreno, 2014). The rise in NPRF taxa continued and culminated at ~1.2 ka, alternating with recurring, centennial-scale increases of *Weinmannia trichosperma* and *Eucryphia/Caldcluvia* paced at millennial timescale. These alternations started at ~6.4 ka and continued until *Eucryphia/Caldcluvia* achieved its final rise at ~0.4 ka. I interpret the onset of centennial-scale shifts in temperature and SWW influence at ~6.4 ka, in agreement with recent findings of enhanced variability in the Chilean Lake District beginning at ~5.4 ka (Moreno and Videla, 2016). This high variability regime led to the alternation of relatively cold/wet and warm/dry centennial-scale intervals, which generated conditions favorable for the development and coexistence of NPRF and VRF communities along the western foothills of the northwestern Patagonian Andes. Subdued fire activity over this interval suggests that the occurrence of centennial-scale warm/dry intervals was insufficient to produce the desiccation and ignition of coarse woody fuels, given the dominant high precipitation regime in the western Andean foothills.

4.3. Regional and hemispheric implications

Ice-free conditions along the Pacific slopes of the northwestern Patagonian Andes commenced at ~17.4 ka (2σ CI: 17.9–17 ka), a statistically indistinguishable age from the radiocarbon chronology for the abandonment of the final LGM margins of multiple glacier lobes in the region (~17.8 ka) (Denton et al., 1999a, 1999b; Moreno et al., 2015). Because Lago Proschle is located near sea level and ~40 km upstream from the LGM margins, I interpret that recession and thinning of the Seno Reloncaví piedmont glacier lobe during T1 was extraordinarily rapid, possibly instantaneous, reaching the western Andean foothills in less than ~400 years. These results underscore the abruptness of glacial withdrawal during T1, probably facilitated by calving of the ice front along the >300-m deep Seno Reloncaví seaway.

Rapid warming during the initial stages of T1, revealed by the abrupt colonization and densification of the temperate rainforest vegetation in areas formerly covered by the Seno Reloncaví glacier lobe, was contemporaneous with the onset of a prominent warming trend initiated shortly after ~18 ka in southeastern Pacific marine records (Haddam et al., 2018; Siani et al., 2013), mountain glaciers in New Zealand's South Island (Barrell et al., 2019; Putnam et al., 2013), and Antarctic ice core records (Stenni et al., 2010) (Fig. 7). This correspondence suggests tight coupling between the middle and high latitudes of the Southern Hemisphere during T1. Poleward shifts of the SWW have been invoked as a fundamental link coupling the hemispheres during ice age terminations, through their effect on the ventilation of CO_2-enriched deep waters to the atmosphere via high-latitude upwelling (Denton et al., 2010). Peak abundance of the paludal Cyperaceae in the Lago Proschle record (~42°S) between ~17.4–16.3 ka was contemporaneous with high abundance of *Isoetes* in the northwestern Patagonian site L. Lepué (~43°S)(Fig. 7), suggesting that low lake levels permitted the

centripetal expansion of littoral environments toward the deepest sectors of these lakes, thereby signaling negative hydrologic balance at ~43°S. One explanation for this diminished SWW influence in northwestern Patagonia is a poleward shift of the SWW between ~17.8 and ~16.3 ka, coeval with the onset of a deglacial rising trend in atmospheric CO_2 (Fig. 7). This correspondence supports the interpretation of enhanced upwelling in the Atlantic sector of the Southern Ocean driven by stronger SWW flow early during T1 (Anderson et al., 2009).

Prominent declines in the percent abundance of Cyperaceae and *Isoetes* in the Lago Proschle and L. Lepué records after ~16.3 ka, respectively (Fig. 7), suggests that a shift toward positive hydrologic balance drove a lake-level rise that forced an outward expansion of littoral environments away from the lake's deepest sectors. This rise in precipitation suggests enhanced SWW influence at latitude ~42°S starting at ~16.3 ka (2σ CI: 16.6–16 ka). I attribute this change to a northward shift of the SWW. This finding replicates similar conclusions drawn from other sites located in the windward side of the Patagonian Andes, where the modern correlation between near-surface SWW speeds and local precipitation are strongly positive (Garreaud et al., 2013; Moreno et al., 2014), these include not only the Lago Lepué, L. Pichilaguna and Canal de la Puntilla sites in northwestern Patagonia (Moreno and Leon, 2003; Moreno et al., 2018a; Pesce and Moreno, 2014) (Fig. 7), but also the L. Edita and L. Unco sites located on the eastern Andean slope of central Chilean Patagonia (Henríquez et al., 2017; Vilanova et al., 2019). Recently, Nanavati et al. (2019) reported synthesis curves for *Nothofagus* pollen percentage and charcoal accumulation rate records from several sites east of the northern, central, and southern Patagonian Andes. Based on these data they inferred vegetation and fire dynamics, human disturbance, paleoclimate changes, and shifts in atmospheric circulation since 18 ka. The extent to which records west and east of the northern Patagonian Andes provide a congruent paleoclimatic history, however, has not been explored in detail in the literature. Physical and biological contrasts are evident between these regions today and are to be expected in paleoclimate reconstructions. More recently, Jara et al. (2019) reported results from Lago Espejo (Fig. 1), a small closed-basin site located in the core region of the northwestern Patagonian Andes, and compared their results with published lake records east and west at that latitude over the last 15,400 years. They concluded that (i) the composition and resilience of *Nothofagus*-dominated forests and scrublands east of the Andean divide affect their paleoclimate-sensing capability, and (ii) the advection of moisture-laden winds from the Atlantic sector toward the eastern Andean slopes may have counteracted the effect of reduced SWW precipitation in the eastern-facing valleys of the northern Patagonian Andes. Additional comparative studies at multiple latitudes across the Andes are necessary to reconcile the similarities and differences in biotic and climatic histories in these contrasting environments.

Vegetation and climate approached average Holocene conditions between ~16.3 and ~15.4 ka, and were followed by prominent increases in the cold-tolerant hygrophilous conifer *Podocarpus nubigena* in Lago Proschle (Fig. 7). One interpretation for this change is that regional climate underwent a cold/wet reversal between ~15.4 and ~12.8 ka that involves increased SWW influence during the Antarctic Cold Reversal (ACR) (Fig. 7). Similar conclusions have been reported from L. Pichilaguna, Huelmo bog, and L. Lepué, using fossil pollen and chironomid records (Massaferro et al., 2009; Moreno and Videla, 2016; Moreno et al., 2018a; Pesce and Moreno, 2014). Likewise, palynologic and glacial geologic evidence from central (Mendelová et al., 2020; Sagredo et al., 2018) and southwestern Patagonia (Garcia et al., 2014; Kaplan et al., 2011; Moreno et al., 2009, 2012; Strelin et al., 2011), both in Chile and Argentina, detected glacier advances and increased influence of the SWW, implying a symmetrical increase in SWW strength from latitudes ~41°S to 52°S during the ACR. The regime shift detection (RSD) analysis (Rodionov, 2004) applied to the *Podocarpus nubigena* records from Lago Proschle (~15.2 ka, 2σ CI: 15.5–15 ka), L. Pichilaguna (14.5 ka, 2σ CI: 15.1–13.9 ka), and the Huelmo bog (~14.8 ka, 2σ CI: 15.3–14.7 ka) (Moreno and Leon, 2003; Moreno et al., 2018a) suggests that the commencement of the ACR signal overlaps at the 95% confidence level (Fig. 8). The latter sites are located in the Longitudinal Valley, ~70 and ~40 km north and northwest of L. Proschle, respectively (Fig. 1). A different situation occurs with the L. Lepué site (~43°S), located ~130 km southwest of L. Proschle in Isla Grande de Chiloé, where the beginning of the ACR signal occurred at ~14.5 ka (2σ CI: 14.8–14.2 ka) according to the RSD algorithm. This age is statistically younger than L. Proschle but the confidence intervals overlap with the chronology of L. Pichilaguna and the Huelmo bog (Fig. 8). If replicated by additional high-resolution precisely dated records, these differences could suggest that residual ice masses in the Andes may have imposed an earlier, large-magnitude cooling signal in the down valley sectors of the northwestern Patagonian Andes through the latter stages of T1. This influence apparently faded westward, as suggested by statistically equivalent ages for the onset of the ACR in sites located in the Longitudinal Valley between ~40 and ~70 km away, and statistically significant differences in a sector from Isla Grande de Chiloé located >100 km from the glaciated Andes.

The Lago Proschle record shows an extraordinarily fast increase in *Weinmannia trichosperma* (Figs. 7 and 8) at the expense of all other trees, concomitant with a sudden rise in fire activity starting at ~12.8 ka (2σ CI: ~12.9–12.6 ka) according to the RSD. Statistically synchronous, nearly identical vegetation changes have been reported from other sites in the Longitudinal Valley of the Chilean Lake District, namely: L. Pichilaguna (~12.3 ka, 2σ CI: 12.6–11.9 ka) and Huelmo bog (~12.7 ka, 2σ CI: 12.9–12.6 ka) (Fig. 8) (Moreno and Leon, 2003; Moreno et al., 2018a). These data indicate a simultaneous response of terrestrial ecosystems to the onset of widespread fire activity in mainland sites from northwestern Patagonia, driven by a decline in summer precipitation at the beginning of the Younger Dryas (YD) chronozone. The L. Lepué pollen record, however, shows that the *W. trichosperma* started at ~11.2 ka (2σ CI: 11.4–10.9 ka), an age statistically younger than the northern sites mentioned above (Fig. 8). One explanation for this difference is that a gradient in rainfall seasonality at the time, evident in the modern climate between these sectors, attenuated the severity, size or frequency of forest fires that acted as a catalyst for the abrupt vegetation changes during YD time in Isla Grande de Chiloé.

Weinmannia trichosperma-dominated assemblages persisted in the Lago Proschle record for ~2500 years followed by a rapid, large-magnitude increase in *Eucryphia/Caldcluvia* at ~10.3 ka (2σ CI: 10.4–10.1 ka) (Fig. 7) according to RSD, which overlaps within confidence intervals with the Huelmo bog (~10.5 ka, 2σ: 10.8–10.4 ka), but took place after L. Pichilaguna (~11.2 ka (2σ CI: 11.3–10.8 ka), (Fig. 8). Altogether these results suggest peak warmth and rainfall seasonality in northwestern Patagonia between ~11.3 and ~7.8 ka. A statistically younger age for the *Eucryphia/Caldcluvia* expansion is evident in the L. Lepué record (~8.8 ka, 2σ CI: 9–8.6 ka), located ~130 km south in Isla Grande de Chiloé (Pesce and Moreno, 2014)(Fig. 8). An explanation involving climatic gradients, rather than migrational lags, is more appropriate to account for the differences in timing for the decisive increments in *Eucryphia/Caldcluvia* in palynological sites located in the mainland and Isla Grande de Chiloé. This is because the *Eucryphia/Caldcluvia* rise in L. Lepué was preceded by a precursor increase between ~10.5 and ~8.8 ka, during which the abundance of this species rose from homogeneously low values with a mean < 0.1% to a highly variable

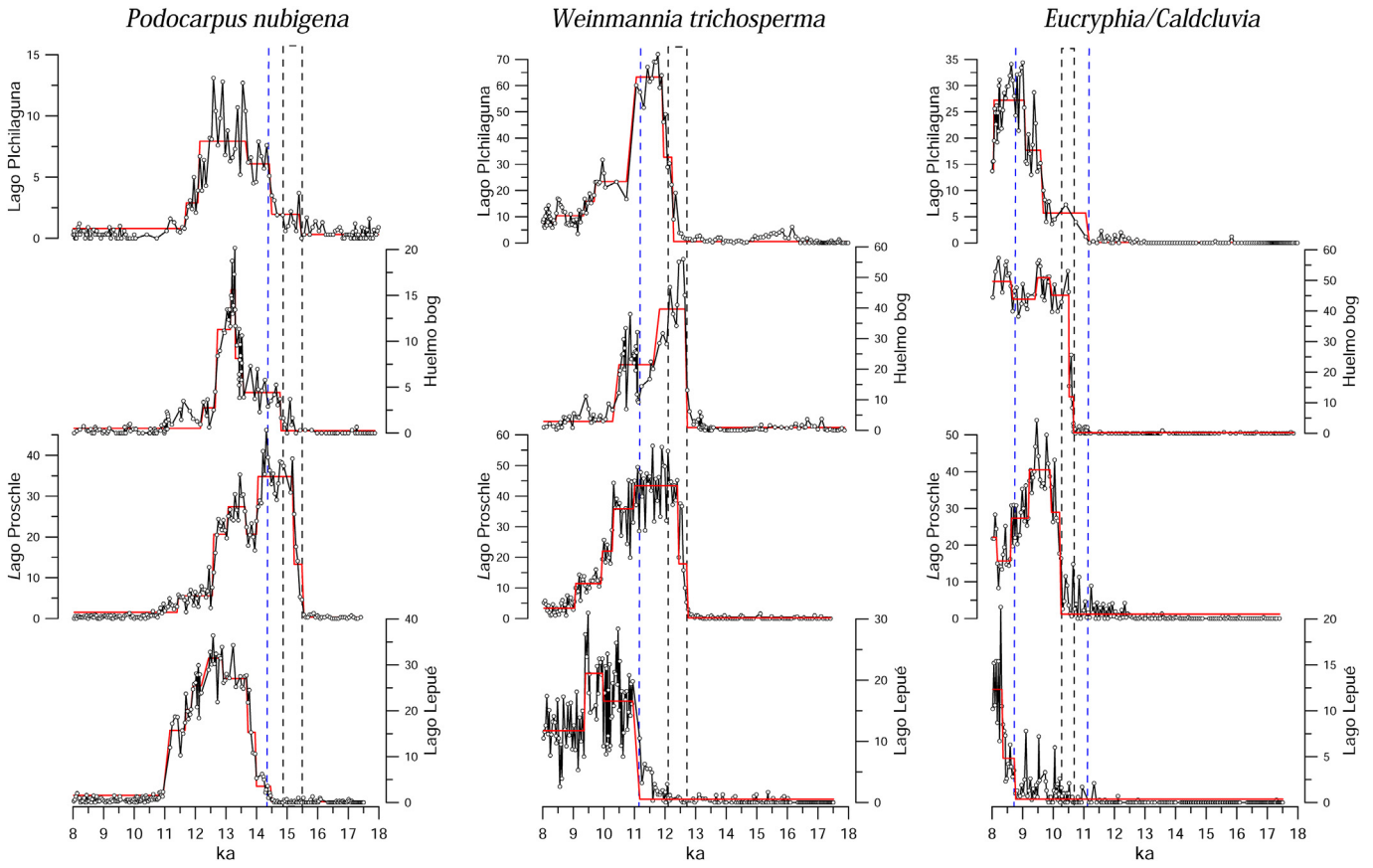

Fig. 8. Comparison of the percent abundance of *Podocarpus nubigena, Weinmannia trichosperma*, and *Eucryphia/Caldcluvia* from Lago Proschle with palynological records from the Longitudinal Valley (L. Pichilaguna, Huelmo bog) and Isla Grande de Chiloé (L. Lepué) sectors from northwestern Patagonia. The records are arranged vertically to reflect their north (top) to south (bottom) position along the latitudinal transect. The percentage data are accompanied by the weighted means of the regimes detected by the RSD algorithm (Rodionov, 2004) using a cutoff length of 10 and a Huber weight function with the tuning constant of 2. Notice the southward increase in the magnitude of *P. nubigena*, pattern that suggests that the modern increase in annual precipitation and decline in annual temperature and precipitation seasonality was also present over this interval. An inverse trend is evident in *W. trichosperma* and *Eucryphia/Caldcluvia* in response to the same climatic gradient. The dashed vertical lines define the age range for the onset of the rising trends for each species among the selected sites, the black lines encompass statistically equivalent modeled ages for the increments, blue lines statistically different ages. (For interpretation of the references to color in this figure legend, the reader is referred to the Web version of this article.)

interval with several peaks >3% (with maxima of 7.8%), and a mean of 1.8%. This precursor increase suggests that *Eucryphia/Caldcluvia* reached the L. Lepué site at least by ~10.5 ka, an age equivalent to the rise observed in mainland sites, and remained in low abundance until favorable environmental conditions permitted its exponential increase at ~8.8 ka. The *Eucryphia/Caldcluvia* rise was contemporaneous with a major increase in *Isoetes* in the L. Lepué record (Fig. 7), signaling a regressive lake-level phase driven by a multi-millennial interval with negative hydrologic balance. I posit that precipitation decreased as the SWW influence at ~42°S declined in successive events starting at the beginning of the YD, and followed by an accentuation that led to an extreme warm/dry phase at the beginning of the Holocene (~11.3–7.8 ka).

The synchronous increments in *Podocarpus nubigena* (~15.4 ka), *Weinmannia trichosperma* (~12.7 ka) and *Eucryphia/Caldcluvia* (~10.3 ka) in Lago Proschle and sites located in the Longitudinal Valley of the Chilean Lake District suggest, within modelled confidence intervals, that physical and climatic barriers did not induce appreciable differences in timing for the establishment of rainforests dominated by these tree species in these sectors. This remarkable synchrony occurs in spite of: (i) the location of L. Proschle ~40 km inboard of the LGM margins (Denton et al., 1999b), (ii) separated from the mainland by the >300 m deep Seno and Estuario Reloncaví seaways , (iii) the inferred persistence of large outlet glaciers in the Estuario Reloncaví and Hornopirén sectors (Davies et al., 2020), and (iv) the occurrence of frequent, large-magnitude explosive volcanic events in this sector since, at least, 18 ka (Alloway et al., 2017). The statistically significant differences in timing for the decisive expansion of *Podocarpus nubigena*, *W. trichosperma* and *Eucryphia/Caldcluvia* between L. Proschle and the Chilotan L. Lepué record (Fig. 8), on the other hand, suggests that north-south and west-east climatic gradients operative through T1 might have delayed the expression of these vegetation signals in central-east Isla Grande de Chiloé. Additional detailed records with precise chronologies from the region will enable assessment of this hypothesis.

A contrast becomes evident when comparing the northwestern Patagonian results with the findings from southwestern Patagonia reported from L. Guanaco, L. Eberhard, and Pantano Dumestre (Moreno et al., 2010, 2012), located ~1100 km south of Lago Proschle. The southern sites indicate an increase in SWW influence (i.e. a rise in precipitation) between ~12.7 and ~11.5 ka, establishing a dipole with the northwestern Patagonian records. I interpret this contrast as a southward shift of the SWW during YD time. A warming pulse and an in-phase decline in precipitation in both regions occurred between ~11.5 and ~7.8 ka, suggesting a

generalized weakening of the SWW throughout Patagonia during the early Holocene (Moreno et al., 2010, 2012, 2018a). This interpretation also applies to paleoclimate records located in other southern mid-latitude landmasses (Fletcher and Moreno, 2011, 2012), implying a zonally symmetric weakening of the SWW during the early Holocene.

The inferred changes in atmospheric circulation patterns are relevant for assessing the postulated role of the SWW as a driver of variations in atmospheric CO_2 concentrations near the end of T1 and the early Holocene. Antarctic ice core records show a conspicuous increase in CO_2 concentrations during YD time that peaked at ~10.5 ka and declined steadily to a minimum at ~7.8 ka (Fig. 8). Our interpreted southward shift of the SWW during YD time would have shifted the focus of SWW influence at or near the critical latitude of the Drake Passage (>56°S), promoting deep upwelling in the Southern Ocean and enhancing high-latitude ventilation of CO_2-rich deep ocean waters. Likewise, weaker-than-present SWW during the early Holocene would reduce the wind stress on the surface of the Southern Ocean, reducing the intensity of upwelling and ventilation of the deep ocean water, thereby accounting for the decline in atmospheric CO_2 concentrations during the early Holocene (Fletcher and Moreno, 2011; Moreno et al., 2010).

The Lago Proschle record suggests a multi-millennial rise in SWW influence that started at ~7.8 ka and has persisted until the present. This shift is also recorded in other northwestern and southwestern Patagonian sites implying a strengthening of the SWW at continental scale, a pattern that is prevalent in other sectors of the middle latitudes of the Southern Hemisphere as well (Fletcher and Moreno, 2011, 2012). Antarctic ice core records reveal a concomitant rise in atmospheric CO_2 concentration from ~7 ka onward (Fig. 7), attesting to a tight coupling between mid- and high-latitude sectors of the Southern Hemisphere through SWW-driven upwelling of deep waters in the Southern Ocean.

I calculated and standardized a ratio between the abundance of *Eucryphia/Caldcluvia* and Podocarpaceae (*Podocarpus nubigena* + *Saxegothaea conspicua*) to express the relative position of a fossil pollen sample from Lago Proschle along a continuum between two endmembers: VRF-dominated (strongly positive anomalies) and NPRF-dominated assemblages (strongly negative anomalies). Fig. 7 shows a comparison of this ratio, or ECPI (*Eucryphia/Caldcluvia* to Podocarpaceae index), with the same parameter calculated from the pollen record from L. Condorito (Moreno, 2004). Both indices exhibit similar multi-millennial trends in vegetation and climate change in northwestern Patagonia: strong negative anomalies during ACR time, a rise during YD time, strong positive anomalies during the early Holocene, and a subsequent decline overprinted by millennial-scale fluctuations until the present. These variations capture the changes in past hydrologic balance discussed above, and are fully coherent with independent estimates of lake level change and fire activity changes in the region (Moreno and Videla, 2016; Pesce and Moreno, 2014; Power et al., 2008; Whitlock et al., 2007), ultimately governed by changes in SWW influence (Moreno et al., 2010)

The SWW became more variable starting at ~6.4 ka, with alternations between relatively warm/dry and cold/wet centennial-scale intervals until the present. The midpoint age for the warm/dry centennial-scale phases in L. Proschle is ~6.4, ~5, ~4.5, ~3.2, ~2.1, ~1, and ~0.4 ka (shown as white triangles in Fig. 5). Moreno and Videla (2016) reported similar results and conclusions from Lago El Salto (Fig. 1), located ~40 km northwest of L. Proschle in the southern portion of the Longitudinal Valley of the Chilean Lake District. The latter record shows conspicuous warm/dry events at centennial timescale centered at ~5.3, ~4.3, ~3.5, ~2.1, ~1.2 ka, and over the last 150 years. Thus, detailed vegetation records from northwestern Patagonia suggest a widespread response of the temperate rainforest vegetation to enhanced, centennial-scale climate variability since ~6.4 ka. Although some events appear to be synchronous within age-model confidence intervals, exact matching of specific events are not to be expected considering that the response capability of a rainforest community is highly dependent upon local contingencies, thresholds, and ecological interactions, which may modulate the precise realization of a climate-driven change in structure and/or rainforest composition. Similar findings have been reported from L. Cipreses (Moreno et al., 2018b), a palynological site located in the mixed evergreen-deciduous *Nothofagus* forest zone of southwestern Patagonia, ~1050 km south of L. Proschle, which shows the commencement of persistent centennial-scale variability at ~5.8 ka, with warm/dry phases centered at ~5.7, ~4.7, ~3.9, ~3.4, ~2.9, ~2.3, ~1.5, ~0.9 ka, and during the last 150 years. Moreno et al. (2018b) attributed these changes to Southern Annular Mode (SAM)-like changes at centennial timescale, considering that SAM is the leading source of climate variability in Patagonian sectors south of ~46°S. Therefore, widespread enhancement of SWW variability throughout Patagonia since ~6.2 ka may represent a regional manifestation of secular SAM-like changes in the southeastern sector of the Pacific Ocean and adjacent South America.

Finally, Lago Proschle record shows disturbance of the vegetation by Chilean/Europeans through the deliberate use of fire since the late 18th century, triggering a trend toward deforestation and proliferation of non-native herbs. The ROC parameter renders this transformation as an abrupt vegetation change, the largest of the last ~12,000 years. This ROC peak surpassed the $+1\sigma$ threshold of the standardized time series during the mid-19th century (Fig. 5), coeval with the establishment of sawmills in the Contao township, a small logging village located 9 km northeast of Lago Proschle. The change in disturbance regimes in this sector included human-set fires, the introduction of cattle, and exploitation of Alerce wood (*Fitzroya cupressoides*). The magnitude of disturbance in the vicinity of Lago Proschle is substantially lower than that observed in palynological sites located in the Longitudinal Valley of the Lake District, e.g. L. Pichilaguna, L. Pichilafquén, and L. El Salto (Jara and Moreno, 2014; Moreno and Videla, 2016; Moreno et al., 2018a). The latter sites document a large-magnitude, nearly instantaneous replacement of the native rainforest vegetation by pasturelands and, to a lesser degree, monospecific plantations of exotic trees. A combination of factors including the age of settlement, road connectivity, population density, intensity of livestock grazing, spread of invasive exotic weeds, and overall drier summers, contributed toward decimation of the native rainforest vegetation in the mainland and a more attenuated impact on the vegetation near L. Proschle.

5. Summary/conclusions

1. Local ice-free conditions started at ~17.4 ka (2σ CI: 17.9–17 ka) along the Pacific slopes of the northwestern Patagonian Andes. Glacier recession during T1 was extraordinarily rapid, possibly instantaneous, reaching the western Andean foothills in less than ~400 years. The abrupt withdrawal of Andean glaciers was driven by warm event at the beginning of T1, probably accelerated by calving of the ice front along the >300-m deep Seno Reloncaví seaway.
2. A brief pioneer phase with cold-tolerant herbs and shrubs typically found in the modern High Andean environments of northwestern Patagonia colonized the barren, newly deglaciated landscapes of the western Andean foothills during the earliest stages of T1.

3. An abrupt vegetation shift led to *Nothofagus*-dominated forests at ~17 ka, accompanied by other cold-tolerant, shade-intolerant, opportunistic tree species characteristic of the modern North Patagonian Rain Forests (NPRF) and abundant ferns.
4. Closed-canopy NPRF with shade-tolerant thermophilous trees established at ~16.3 ka, implying a culmination of the warming trend that initiated T1. This event was preceded by an increase in precipitation I attribute to a northward shift in the SWW that terminated an interval with diminished precipitation at ~42°S, dated between ~17.4 and ~16.3 ka.
5. A reversal to cold conditions occurred between ~15.4 and ~12.8 ka, during the Antarctic Cold Reversal, implied by the dominance of *Nothofagus*, cold-tolerant hygrophilous conifers, and absence of fires. This change was coupled with increased SWW influence in the region, probably representing a northward shift of this wind belt.
6. A sudden decline in summer precipitation and warmer summers started at ~12.8 ka, at the onset of the Younger Dryas, implied by stand-replacing fires, proliferation of trees favored by disturbance, and disappearance of moisture-demanding shade-tolerant trees. The rates of vegetation associated with this transition were extraordinarily fast, the highest of the entire Lago Proschle record. I interpret a decline in SWW influence in the region, probably representing a southward shift of this wind belt.
7. Peak warmth and overall decline in annual precipitation brought by maximum rainfall seasonality occurred between ~10.3 and 7.8 ka, implied by the dominance of thermophilous, summer-drought tolerant Valdivian rainforest trees and high fire activity. These results are consistent with a zonally symmetric weakening of the SWW during the early Holocene.
8. A multi-millennial cooling and wetting phase started at ~7.8 ka, shown by decline in VRF trees, rise in NPRF trees, and decline in fire activity, implying a strengthening of the SWW at continental and zonal scale. This widespread and stronger SWW influence was contemporaneous with a rise in atmospheric CO_2 concentrations in Antarctic ice cores.
9. The SWW became more variable starting at ~6.4 ka, with alternations between relatively warm/dry and cold/wet centennial-scale intervals until the present.
10. Deforestation and spread of non-native herbs commenced during the late 18th century, caused by the deliberate use of fire by historical settling. This transformation was abrupt, being the largest magnitude event of the last ~12,000 years in the Lago Proschle record.
11. Our results suggest that physical and climatic barriers did not induce appreciable delays in the establishment of selected rainforest taxa in the northern portion of Chiloé Continental, relative to the Longitudinal Valley of the Chilean Lake District, during and following T1.

Acknowledgements

I thank M.-S. Fletcher, R. Flores, R. Villa, and A. Westermeyer for help during field work, L. Hernández and M. Valenzuela for laboratory assistance, E. Fercovic for drafting Fig. 1, and T. Guilderson, S. Collado and R. De Pol for analyzing the radiocarbon samples. I acknowledge funding from Fondecyt 1191435 and the ANID Millennium Science Initiative/Millennium Nucleus Paleoclimate NCN17_079.

References

Aceituno, P., Fuenzalida, H., Rosenbluth, 1993. Climate along the extratropical west coast of South America. In: Mooney, Fuentes, Kromberg (Eds.), Earth Systems Responses to Global Change. Academic press, pp. 61–70.
Agosta, E., Compagnucci, R., Ariztegui, D., 2015. Precipitation linked to Atlantic moisture transport: clues to interpret Patagonian palaeoclimate. Clim. Res. 62, 219–240.
Alloway, B.V., Pearce, N.J.G., Moreno, P.I., Villarosa, G., Jara, I., De Pol-Holz, R., Outes, V., 2017. An 18,000 year-long eruptive record from Volcán Chaitén, northwestern Patagonia: paleoenvironmental and hazard-assessment implications. Quat. Sci. Rev. 168, 151–181.
Anderson, R.F., Ali, S., Bradtmiller, L.I., Nielsen, S.H.H., Fleisher, M.Q., Anderson, B.E., Burckle, L.H., 2009. Wind-driven upwelling in the Southern Ocean and the deglacial rise in atmospheric CO2. Science 323, 1443–1448.
Barrell, D.J.A., Putnam, A.E., Denton, G.H., 2019. Reconciling the onset of deglaciation in the upper Rangitata valley, Southern Alps, New Zealand. Quat. Sci. Rev. 203, 141–150.
Blaauw, M., Christen, J.A., 2011. Flexible paleoclimate age-depth models using an autoregressive gamma process. Bayesian Anal. 6, 457–474.
Davies J., Bethan, Darvill M., C., Lovell, H., Bendle M., J., Dowdeswell A., J., Fabel, D., García L., J., Geiger, A., Glasser F., N., Gheorghiu M., D., Harrison, S., Hein S., A., Kaplan R., M., Martin R., J., Mendelova, M., Palmer, A., Pelto, M., Rodés, A., Sagredo A., E., Smedley K., R., Smellie L., J., Thorndycraft R., V., et al., 2020. The evolution of the Patagonian Ice Sheet from 35 ka to the present day (PATICE). Earth-Sci. Rev. 204, 103152. https://doi.org/10.1016/j.earscirev.2020.103152.
Denton, G.H., Anderson, R.F., Toggweiler, J.R., Edwards, R.L., Schaefer, J.M., Putnam, A.E., 2010. The last glacial termination. Science 328, 1652–1656.
Denton, G.H., Heusser, C.J., Lowell, T.V., Moreno, P.I., Andersen, B.G., Heusser, L.E., Schluchter, C., Marchant, D.R., 1999a. Interhemispheric linkage of paleoclimate during the last glaciation. Geogr. Ann. Phys. Geogr. 81A, 107–153.
Denton, G.H., Lowell, T.V., Heusser, C.J., Schluchter, C., Andersen, B.G., Heusser, L.E., Moreno, P.I., Marchant, D.R., 1999b. Geomorphology, stratigraphy, and radiocarbon chronology of Llanquihue drift in the area of the southern Lake District, Seno reloncavi, and Isla Grande de Chiloe, Chile. Geogr. Ann. Phys. Geogr. 81A, 167–229.
Faegri, K., Iversen, J., 1989. Textbook of Pollen Analysis. John Wiley & Sons.
Figueroa, J.A., Lusk, C.H., 2001. Germination requirements and seedling shade tolerance are not correlated in a Chilean temperate rain forest. New Phytol. 152, 483–489.
Fletcher, M.-S., Moreno, P.I., 2011. Zonally symmetric changes in the strength and position of the Southern Westerlies drove atmospheric CO2 variations over the past 14 k. y. Geology 39, 419–422.
Fletcher, M.S., Moreno, P.I., 2012. Have the Southern Westerlies changed in a zonally symmetric manner over the last 14,000 years? A hemisphere-wide take on a controversial problem. Quat. Int. 253, 32–46.
Fontijn, K., Lachowycz, S.M., Rawson, H., Pyle, D.M., Mather, T.A., Naranjo, J.A., Moreno-Roa, H., 2014. Late Quaternary tephrostratigraphy of southern Chile and Argentina. Quat. Sci. Rev. 89, 70–84.
Garcia, J.L., Hall, B.L., Kaplan, M.R., Vega, R.M., Strelin, J.A., 2014. Glacial geomorphology of the Torres del Paine region (southern Patagonia): implications for glaciation, deglaciation and paleolake history. Geomorphology 204, 599–616.
Garreaud, R., Lopez, P., Minvielle, M., Rojas, M., 2013. Large-scale control on the patagonian climate. J. Clim. 26, 215–230.
Grimm, E.C., 1987. CONISS: a FORTRAN 77 program for stratigraphically constrained cluster analysis by the method of incremental sum of squares. Comput. Geosci. 13, 13–35.
Grimm, E.C., Jacobson, G.L., 1992. Fossil-pollen evidence for abrupt climatic changes during the past 18,000 years in eastern North America. Clim. Dynam. 6, 179–184.
Haddam, N.A., Siani, G., Michel, E., Kaiser, J., Lamy, F., Duchamp-Alphonse, S., Hefter, J., Braconnot, P., Dewilde, F., Isgüder, G., Tisnerat-Laborde, N., Thil, F., Durand, N., Kissel, C., 2018. Changes in latitudinal sea surface temperature gradients along the Southern Chilean margin since the last glacial. Quat. Sci. Rev. 194, 62–76.
Heiri, O., Lotter, A.F., Lemcke, G., 2001. Loss on ignition as a method for estimating organic and carbonate content in sediments: reproducibility and comparability of results. J. Paleolimnol. 25, 101–110.
Henríquez, W.I., Moreno, P.I., Alloway, B.V., Villarosa, G., 2015. Vegetation and climate change, fire-regime shifts and volcanic disturbance in Chiloé Continental (43°S) during the last 10,000 years. Quat. Sci. Rev. 123, 158–167.
Henríquez, W.I., Villa-Martínez, R., Vilanova, I., De Pol-Holz, R., Moreno, P.I., 2017. The last glacial termination on the eastern flank of the central Patagonian Andes (47 °S). Clim. Past 13, 879–895.
Heusser, C.J., 1966. Late-Pleistocene pollen diagrams from the Province of Llanquihue, southern Chile. Proc. Am. Phil. Soc. 110, 269–305.
Heusser, C.J., 1971. Pollen and Spores from Chile. University of Arizona Press, Tucson.
Heusser, C.J., 1974. Vegetation and climate of the southern Chilean lake district during and since the last Interglaciation. Quat. Res. 4, 190–315.
Heusser, C.J., 1984. Late-glacial-Holocene climate of the lake district of Chile. Quat. Res. 22, 77–90.
Heusser, C.J., Denton, G.H., Hauser, A., Andersen, B.G., Lowell, T.V., 1995. Quaternary pollen records from the Archipiélago de Chiloé in the context of glaciation and

climate. Rev. Geol. Chile 22, 25–46.
Heusser, C.J., Heusser, L.E., Hauser, A., 1992. Paleoecology OF late quaternary deposits IN chiloe continental, Chile. Rev. Chil. Hist. Nat. 65, 235–245.
Heusser, C.J., Heusser, L.E., Lowell, T.V., 1999. Paleoecology of the southern Chilean Lake District- Isla Grande de Chiloé during middle-late Llanquihue glaciation and deglaciation. Geogr. Ann. Phys. Geogr. 81 A, 231–284.
Heusser, C.J., Lowell, T.V., Heusser, L.E., Hauser, A., Andersen, B.G., Denton, G.H., 1996a. Full-glacial - late-glacial palaeoclimate of the Southern Andes: evidence from pollen, beetle, and glacial records. J. Quat. Sci. 11, 173–184.
Heusser, C.J., Lowell, T.V., Heusser, L.E., Hauser, A., Andersen, B.G., Denton, G.H., 1996b. Vegetation dynamics and paleoclimate during late Llanquihue glaciation in Southern Chile. Bamb. Geogr. Schriften 15, 201–218.
Higuera, P.E., Brubaker, L.B., Anderson, P.M., Hu, F.S., Brown, T.A., 2009. Vegetation mediated the impacts of postglacial climate change on fire regimes in the south-central Brooks Range, Alaska. Ecol. Monogr. 79, 201–219.
Hogg, A.G., Hua, Q., Blackwell, P.G., Niu, M., Buck, C.E., Guilderson, T.P., Heaton, T.J., Palmer, J.G., Reimer, P.J., Reimer, R.W., Turney, C.S.M., Zimmerman, S.R.H., 2013. SHCal13 southern hemisphere calibration, 0–50,000 Years cal BP. Radiocarbon 55, 1889–1903.
Holz, A., Veblen, T.T., 2012. Wildfire activity in rainforests in western Patagonia linked to the southern annular Mode. Int. J. Wildland Fire 21, 114–126.
Jacobson, G.L.J., Webb, T.I., Grimm, E.C., 1987. Patterns and rates of vegetation change during the deglaciation of eastern North America. In: Ruddiman, W.F., Wright, H.E.J. (Eds.), North America during Deglaciation. Geological Society of America, Boulder, CO, USA, pp. 277–288.
Jara, I.A., Moreno, P.I., 2014. Climatic and disturbance influences on the temperate rainforests of northwestern Patagonia (40 °S) since ~14,500 cal yr BP. Quat. Sci. Rev. 90, 217–228.
Jara, I.A., Moreno, P.I., Alloway, B.V., Newnham, R.M., 2019. A 15,400-year long record of vegetation, fire-regime, and climate changes from the northern Patagonian Andes. Quat. Sci. Rev. 226, 106005.
Kaplan, M.R., Strelin, J.A., Schaefer, J.M., Denton, G.H., Finkel, R.C., Schwartz, R., Putnam, A.E., Vandergoes, M.J., Goehring, B.M., Travis, S.G., 2011. In-situ cosmogenic 10Be production rate at Lago Argentino, Patagonia: implications for late-glacial climate chronology. Earth Planet Sci. Lett. 309, 21–32.
Lamy, F., Hebbeln, D., Wefer, G., 1999. High-resolution marine record of climatic change in mid-latitude Chile during the last 28,000 Years based on terrigenous sediment parameters. Quat. Res. 51, 83–93.
Lara, A., Villalba, R., Wolodarsky-Franke, A., Aravena, J.C., Luckman, B.H., Cuq, E., 2005. Spatial and temporal variation in Nothofagus pumilio growth at tree line along its latitudinal range (35 degrees 40 '-55 degrees S) in the Chilean Andes. J. Biogeogr. 32, 879–893.
Lliboutry, L., 1998. Glaciers of Chile and Argentina. In: Williams, R.S., Ferrigno, J.G. (Eds.), Satellite Image Atlas of Glaciers of the World: South America. USGS Professional Paper 1386-I, Online Version 1.02.
Markgraf, V., 1991. Younger Dryas in south America? Boreas 20, 63–69.
Massaferro, J.I., Moreno, P.I., Denton, G.H., Vandergoes, M., Dieffenbacher-Krall, A., 2009. Chironomid and pollen evidence for climate fluctuations during the last glacial termination in NW Patagonia. Quat. Sci. Rev. 28, 517–525.
Mendelová, M., Hein, A.S., Rodés, Á., Smedley, R.K., Xu, S., 2020. Glacier expansion in central Patagonia during the antarctic cold reversal followed by retreat and stabilisation during the younger Dryas. Quat. Sci. Rev. 227, 106047.
Moreno, P.I., 1997. Vegetation and climate near Lago Llanquihue in the Chilean Lake District between 20200 and 9500 C-14 yr BP. J. Quat. Sci. 12, 485–500.
Moreno, P.I., 2004. Millennial-scale climate variability in northwest Patagonia over the last 15000 yr. J. Quat. Sci. 19, 35–47.
Moreno, P.I., Denton, G.H., Moreno, H., Lowell, T.V., Putnam, A.E., Kaplan, M.R., 2015. Radiocarbon chronology of the last glacial maximum and its termination in northwestern Patagonia. Quat. Sci. Rev. 122, 233–249.
Moreno, P.I., Francois, J.P., Villa-Martínez, R., Moy, C.M., 2010. Covariability of the southern westerlies and atmospheric CO2 during the Holocene. Geology 39, 727–730.
Moreno, P.I., Jacobson, G.L., Andersen, B.G., Lowell, T.V., Denton, G.H., 1999. Abrupt vegetation and climate changes during the last glacial maximum and the last Termination in the Chilean Lake District: a case study from Canal de la Puntilla (41°S). Geogr. Ann. Phys. Geogr. 81 A, 285–311.
Moreno, P.I., Kaplan, M.R., Francois, J.P., Villa-Martinez, R., Moy, C.M., Stern, C.R., Kubik, P.W., 2009. Renewed glacial activity during the Antarctic cold reversal and persistence of cold conditions until 11.5 ka in southwestern Patagonia. Geology 37, 375–378.
Moreno, P.I., Leon, A.L., 2003. Abrupt vegetation changes during the last glacial to Holocene transition in mid-latitude South America. J. Quat. Sci. 18, 787–800.
Moreno, P.I., Videla, J., 2016. Centennial and millennial-scale hydroclimate changes in northwestern Patagonia since 16,000 yr BP. Quat. Sci. Rev. 149, 326–337.
Moreno, P.I., Videla, J., Valero-Garcés, B., Alloway, B.V., Heusser, L.E., 2018a. A continuous record of vegetation, fire-regime and climatic changes in northwestern Patagonia spanning the last 25,000 years. Quat. Sci. Rev. 198, 15–36.
Moreno, P.I., Vilanova, I., Villa-Martínez, R., Dunbar, R.B., Mucciarone, D.A., Kaplan, M.R., Garreaud, R.D., Rojas, M., Moy, C.M., Pol-Holz, R.D., Lambert, F., 2018b. Onset and evolution of southern annular mode-like changes at centennial timescale. Sci. Rep. 8, 3458.
Moreno, P.I., Vilanova, I., Villa-Martínez, R., Garreaud, R.D., Rojas, M., De Pol-Holz, R., 2014. Southern Annular Mode-like changes in southwestern Patagonia at centennial timescales over the last three millennia. Nat. Commun. 5, 4375.
Moreno, P.I., Villa-Martinez, R., Cardenas, M.L., Sagredo, E.A., 2012. Deglacial changes of the southern margin of the southern westerly winds revealed by terrestrial records from SW Patagonia (52 degrees S). Quat. Sci. Rev. 41, 1–21.
Nanavati, W.P., Whitlock, C., Iglesias, V., de Porras, M.E., 2019. Postglacial vegetation, fire, and climate history along the eastern Andes, Argentina and Chile (lat. 41–55°S). Quat. Sci. Rev. 207, 145–160.
Palacios, D., Stokes R., C., Phillips M., F., Clague J., J., Alcalá-Reygosa, J., Andrés, N., Angel, I., Blard, P.-H., Briner P., J., Hall L., B., Dahms, D., Hein S., A., Jomelli, V., Mark G., B., Martini A., M., Moreno I., P., Riedel, J., Sagredo, E., Stansell D., N., Vázquez-Selem, L., Vuille, M., Ward J., D., et al., 2020. The deglaciation of the Americas during the Last Glacial Termination. Earth-Science Rev. 203, 103113. https://doi.org/10.1016/j.earscirev.2020.103113.
Pesce, O.H., Moreno, P.I., 2014. Vegetation, fire and climate change in central-east Isla Grande de Chiloé (43°S) since the last glacial maximum, northwestern Patagonia. Quat. Sci. Rev. 90, 143–157.
Power, M.J., Marlon, J., Ortiz, N., Bartlein, P.J., Harrison, S.P., Mayle, F.E., Ballouche, A., Bradshaw, R.H.W., Carcaillet, C., Cordova, C., Mooney, S., Moreno, P.I., Prentice, I.C., Thonicke, K., Tinner, W., Whitlock, C., Zhang, Y., Zhao, Y., Ali, A.A., Anderson, R.S., Beer, R., Behling, H., Briles, C., Brown, K.J., Brunelle, A., Bush, M., Camill, P., Chu, G.Q., Clark, J., Colombaroli, D., Connor, S., Daniau, A.L., Daniels, M., Dodson, J., Doughty, E., Edwards, M.E., Finsinger, W., Foster, D., Frechette, J., Gaillard, M.J., Gavin, D.G., Gobet, E., Haberle, S., Hallett, D.J., Higuera, P., Hope, G., Horn, S., Inoue, J., Kaltenrieder, P., Kennedy, L., Kong, Z.C., Larsen, C., Long, C.J., Lynch, J., Lynch, E.A., McGlone, M., Meeks, S., Mensing, S., Meyer, G., Minckley, T., Mohr, J., Nelson, D.M., New, J., Newnham, R., Noti, R., Oswald, W., Pierce, J., Richard, P.J.H., Rowe, C., Goni, M.F.S., Shuman, B.N., Takahara, H., Toney, J., Turney, C., Urrego-Sanchez, D.H., Umbanhowar, C., Vandergoes, M., Vanniere, B., Vescovi, E., Walsh, M., Wang, X., Williams, N., Wilmshurst, J., Zhang, J.H., 2008. Changes in fire regimes since the Last Glacial Maximum: an assessment based on a global synthesis and analysis of charcoal data. Clim. Dynam. 30, 887–907.
Putnam, A.E., Schaefer, J.M., Denton, G.H., Barrell, D.J.A., Andersen, B.G., Koffman, T.N.B., Rowan, A.V., Finkel, R.C., Rood, D.H., Schwartz, R., Vandergoes, M.J., Plummer, M.A., Brocklehurst, S.H., Kelley, S.E., Ladig, K.L., 2013. Warming and glacier recession in the rakaia valley, southern alps of New Zealand, during heinrich stadial 1. Earth Planet Sci. Lett. 382, 98–110.
Quintana, J.M., Aceituno, P., 2012. Changes in the rainfall regime along the extratropical west coast of South America (Chile): 30-43 degrees S. Atmósfera 25, 1–22.
Reimer, P.J., Bard, E., Bayliss, A., Beck, J.W., Blackwell, P.G., Ramsey, C.B., Buck, C.E., Cheng, H., Edwards, R.L., Friedrich, M., Grootes, P.M., Guilderson, T.P., Haflidason, H., Hajdas, I., Hatté, C., Heaton, T.J., Hoffmann, D.L., Hogg, A.G., Hughen, K.A., Kaiser, K.F., Kromer, B., Manning, S.W., Niu, M., Reimer, R.W., Richards, D.A., Scott, E.M., Southon, J.R., Staff, R.A., Turney, C.S.M., van der Plicht, J., 2013. IntCal13 and Marine13 radiocarbon age calibration curves 0–50,000 Years cal BP. Radiocarbon 55, 1869–1887.
Rodionov, S.N., 2004. A sequential algorithm for testing climate regime shifts. Geophys. Res. Lett. 31.
Rodrigo, C., 2006a. Caracterización y clasificación de la bahía de Puerto Montt mediante batimetría de multihaz y datos de backscatter. Invest. Mar. 34, 83–94.
Rodrigo, C., 2006b. Topografía submarina en canales de la Patagonia Norte. In: Silva, N., Palma, S. (Eds.), Avances en el conocimiento oceanográfico de las aguas interiores chilenas, Puerto Montt a cabo de Hornos. Comité Oceanográfico Nacional - Pontificia Universidad Católica de Valparaíso, Valparaiso, p. 160.
Sagredo, E.A., Kaplan, M.R., Araya, P.S., Lowell, T.V., Aravena, J.C., Moreno, P.I., Kelly, M.A., Schaefer, J.M., 2018. Trans-pacific glacial response to the Antarctic Cold Reversal in the southern mid-latitudes. Quat. Sci. Rev. 188, 160–166.
Siani, G., Michel, E., De Pol-Holz, R., DeVries, T., Lamy, F., Carel, M., Isguder, G., Dewilde, F., Lourantou, A., 2013. Carbon isotope records reveal precise timing of enhanced Southern Ocean upwelling during the last deglaciation. Nat. Commun. 4.
Stenni, B., Masson-Delmotte, V., Selmo, E., Oerter, H., Meyer, H., Rothlisberger, R., Jouzel, J., Cattani, O., Falourd, S., Fischer, H., Hoffmann, G., Iacumin, P., Johnsen, S.J., Minster, B., Udisti, R., 2010. The deuterium excess records of EPICA Dome C and Dronning Maud Land ice cores (East Antarctica). Quat. Sci. Rev. 29, 146–159.
Stern, C., 2004. Active Andean volcanism: its geologic and tectonic setting. Rev. Geol. Chile 31, 161–206.
Strelin, J.A., Denton, G.H., Vandergoes, M.J., Ninnemann, U.S., Putnam, A.E., 2011. Radiocarbon chronology of the late-glacial Puerto bandera moraines, southern patagonian icefield, Argentina. Quat. Sci. Rev. 30, 2551–2569.
Vilanova, I., Moreno, P.I., Miranda, C.G., Villa-Martínez, R.P., 2019. The last glacial termination in the Coyhaique sector of central Patagonia. Quat. Sci. Rev. 224, 105976.
Villagrán, C., 1980. Vegetatiosgeschichtliche und pflanzensoziologische Untersuchungen im Vicente Perez Rosales Nationalpark (Chile). Diss. Bot. 54, 1–165.
Villagrán, C., 1985. Análisis palinológico de los cambios vegetacionales durante el Tardiglacial y Postglacial en Chiloé, Chile. Rev. Chil. Hist. Nat. 58, 57–69.
Villagrán, C., 1988a. Expansion of magellanic moorland during the late pleistocene: palynological evidence from northern Isla Grande de Chiloé, Chile. Quat. Res. 30, 304–314.
Villagrán, C., 1988b. Late quaternary vegetation of southern Isla Grande de Chiloé, Chile. Quat. Res. 29, 294–306.
Villagrán, C., 1990. Glacial, late-glacial, and post-glacial climate and vegetation of the Isla Grande de Chiloé, southern Chile (41-44°s). Quat. S. Am. Antarct. Peninsula 8, 1–15.

Villagrán, C., 2001. Un modelo de la historia de la vegetación de la Cordillera de la Costa de Chile central-sur: la hipótesis glacial de Darwin. Rev. Chil. Hist. Nat. 74, 793–803.
Villalba, R., Lara, A., Masiokas, M.H., Urrutia, R., Luckman, B.H., Marshall, G.J., Mundo, I.A., Christie, D.A., Cook, E.R., Neukom, R., Allen, K., Fenwick, P., Boninsegna, J.A., Srur, A.M., Morales, M.S., Araneo, D., Palmer, J.G., Cuq, E., Aravena, J.C., Holz, A., LeQuesne, C., 2012. Unusual southern hemisphere tree growth patterns induced by changes in the southern annular Mode. Nat. Geosci. 5, 793–798.
Whitlock, C., Anderson, R.S., 2003. Fire history reconstructions based on sediment records from lakes and wetlands. In: Veblen, T.T., Baker, W.L., Montenegro, G., Swetnam, T.W. (Eds.), Fire and Climatic Change in Temperate Ecosystems of the Western Americas. Springer, New York, pp. 265–295.
Whitlock, C., Moreno, P.I., Bartlein, P., 2007. Climatic controls of Holocene fire patterns in southern South America. Quat. Res. 68, 28–36.